

Article

Strength of the $[Z-I\cdots Hal]^-$ and $[Z-Hal\cdots I]^-$ Halogen Bonds: Electron Density Properties and Halogen Bond Length as Estimators of Interaction Energy

Maxim L. Kuznetsov ^{1,2} 

¹ Centro de Química Estrutural, Instituto Superior Técnico, Universidade de Lisboa, Avenida Rovisco Pais, 1049-001 Lisbon, Portugal; max@mail.ist.utl.pt; Tel.: +351-218-419-236

² Institute of Chemistry, Saint Petersburg State University, Universitetskaya Nab. 7/9, 199034 Saint Petersburg, Russia

Abstract: Bond energy is the main characteristic of chemical bonds in general and of non-covalent interactions in particular. Simple methods of express estimates of the interaction energy, E_{int} , using relationships between E_{int} and a property which is easily accessible from experiment is of great importance for the characterization of non-covalent interactions. In this work, practically important relationships between E_{int} and electron density, its Laplacian, curvature, potential, kinetic, and total energy densities at the bond critical point as well as bond length were derived for the structures of the $[Z-I\cdots Hal]^-$ and $[Z-Hal\cdots I]^-$ types bearing halogen bonds and involving iodine as interacting atom(s) (totally 412 structures). The mean absolute deviations for the correlations found were 2.06–4.76 kcal/mol.

Keywords: bond critical point properties; interaction energy; bond energy; bond strength; density functional theory; electron density; energy density; halogen bond; QTAIM



Citation: Kuznetsov, M.L. Strength of the $[Z-I\cdots Hal]^-$ and $[Z-Hal\cdots I]^-$ Halogen Bonds: Electron Density Properties and Halogen Bond Length as Estimators of Interaction Energy. *Molecules* **2021**, *26*, 2083. <https://doi.org/10.3390/molecules26072083>

Academic Editor: James Gault

Received: 26 February 2021

Accepted: 31 March 2021

Published: 5 April 2021

Publisher's Note: MDPI stays neutral with regard to jurisdictional claims in published maps and institutional affiliations.



Copyright: © 2021 by the author. Licensee MDPI, Basel, Switzerland. This article is an open access article distributed under the terms and conditions of the Creative Commons Attribution (CC BY) license (<https://creativecommons.org/licenses/by/4.0/>).

1. Introduction

The halogen bond is one of the most important types of non-covalent interactions being second only to hydrogen bonds in its significance. According to the IUPAC definition, “a halogen bond occurs when there is evidence of a net attractive interaction between an electrophilic region associated with a halogen atom in a molecular entity and a nucleophilic region in another, or the same, molecular entity” [1]. Weak interactions in general and halogen bonds in particular underly the self-assembly strategy [2–4] leading to new functional materials [5–17] and are applied in crystal engineering [15], catalysis [18–20], and drug design [21–23].

The supramolecular and cluster chemistry of halide anions currently attracts much attention [24–29] due to their important role in chemistry and biology [30–33]. Halogen bonds formed by a halide anion belong to a particularly interesting type of non-covalent interactions. They play a key role in the design of chemical receptors for anion recognition [27,34–38], in the anion-assisted asymmetric catalysis [39–42], and in the development of approaches toward new materials bearing useful electronic properties [43–50].

Properties of functional materials and supramolecular structures formed by halogen bonding are controlled by its strength. Therefore, halogen bond energy is the most important characteristic of these interactions. However, determination of the bond energy (E_b) is a difficult task. Experimental methods (e.g., mass spectrometry, vibrational or NMR spectroscopy, calorimetry, vapor density measurements) are usually associated with complex technical procedures and can be applied to a very limited number of structures. The direct theoretical calculations of E_b for the $A\cdots B$ bond as the energy difference between the structure $A\cdots B$ and the isolated molecules A and B may be successfully applied to intermolecular non-covalent interactions in the gas phase. However, in the condensed

phase, molecules are usually bound with each other by a network of several non-covalent interactions, and an adequate fragmentation which affects only the bond of interest is often impossible. In such a situation, an approximation of E_b through other parameters easily accessible from experiment becomes very important [51–60]. Among these parameters, bond distance [61–78], electron density properties [61,79–113], and force constants [57,73,114,115] are the most common. In fact, the application of E_b -property relationships is often the only possibility to estimate the energy of non-covalent interactions in the condensed phase.

A broad practical utilization of the E_b -property relationships for the estimates of E_b started with a publication by Espinosa, Molins, and Lecomte [82], where a simple correlation between the bond energy and the potential energy density (V_b) at the bond critical point (BCP) was obtained for the X–H···O hydrogen bonds (X = C, N, O):

$$E_{\text{int}} \sim 0.5V_b$$

where E_{int} is the interaction energy of the A···B bond defined as $E_{\text{int}} = E_{A\cdots B} - E_A - E_B$ (A and B are fragments with unrelaxed geometry corresponding to the structure A···B). Later, several other equations for the approximation of E_{int} through the electron density properties were published for hydrogen and halogen bonds (Table 1 and Table S1). Meanwhile, it was shown that these relationships are not universal and may be applied only to the type of interaction for which they were derived [116–118].

Table 1. Relationships between interaction energy (E_{int} , kcal/mol) and potential or kinetic energy density (V_b or G_b , kcal/(mol•bohr³)).

| Type of Interaction | Estimator | Relationship | Reference |
|---------------------|-----------|--|-----------|
| H···O | V_b | $E_{\text{int}} \sim 0.5V_b$ | [82] |
| FH···FR | G_b | $E_{\text{int}} \sim -0.429G_b$ | [83,86] |
| | V_b | $E_{\text{int}} \sim 0.37V_b - 3.1$ | [83] |
| Cl···X ^a | V_b | $E_{\text{int}} \sim 0.49V_b$ | [119] |
| | G_b | $E_{\text{int}} \sim -0.47G_b$ | [119] |
| Br···X ^a | V_b | $E_{\text{int}} \sim 0.58V_b$ | [119] |
| | V_b | $E_{\text{int}} \sim 0.375V_b - 0.57$ | [120] |
| | G_b | $E_{\text{int}} \sim -0.57G_b$ | [119] |
| I···X ^a | V_b | $E_{\text{int}} \sim 0.68V_b$ | [119] |
| | V_b | $E_{\text{int}} \sim 0.556V_b + 0.64$ | [120] |
| | G_b | $E_{\text{int}} \sim -0.67G_b$ | [119] |
| F···F | G_b | $E_{\text{int}} \sim -0.129G_b$ | [87] |
| Cl···Cl | V_b | $E_{\text{int}} \sim -0.1006V_b^2 - 0.218V_b - 0.55$ | [117] |
| | G_b | $E_{\text{int}} \sim -0.0841G_b^2 + 0.367G_b - 0.84$ | [117] |
| Br···Br | V_b | $E_{\text{int}} \sim -0.0926V_b^2 - 0.173V_b - 0.16$ | [117] |
| | G_b | $E_{\text{int}} \sim -0.1178G_b^2 + 0.73G_b - 1.5$ | [117] |
| I···I | V_b | $E_{\text{int}} \sim -0.0635V_b^2 - 0.217V_b - 0.25$ | [117] |
| | G_b | $E_{\text{int}} \sim -0.1564G_b^2 + 1.138G_b - 2.25$ | [117] |

^a X = N, S, O, C in [119], X = O, N, F in [120].

Recently, the author started a project to establish practically useful correlations between the interaction energy and properties which could be easily determined from experiment for halogen bonds of various types, including those formed by a halide anion. In the previous work [116], such relationships were found for structures of the [(A)_nZ–Y···X][−] type (X, Y = F, Cl, Br; Z = F, Cl, Br, C, N, O, H, S, P, Si, B; 441 structures in total). The aim of this work was to include in the consideration the structures bearing the interacting iodine atom(s), thus completing the whole series of halogen bonds with a halide anion. In this work, structures of the [(A)_nZ–I···X][−] and [(A)_nZ–Y···I][−] types (X = F, Cl, Br, I; Y = Cl, Br, I; Z = F, Cl, Br, I, C, N, O, H, S, P, Si, B) were calculated. The correlations between E_{int} and the electron density (ρ_b), its Laplacian ($\nabla^2\rho_b$), the curvature of $\rho(r)$ which is parallel to the bond path direction (positive) ($\lambda_{||,b}$), the potential, kinetic, and total energy densities (V_b , G_b , and H_b) at BCP, and the halogen bond length ($d_{Y\cdots X}$) were established.

Two points should be mentioned here. First, the interactions with the iodine atom as a halogen bond donor are the most important among all halogen bonds since the existence of a prominent σ -hole at the iodine atom provides particularly high stability of these interactions. Second, reliable relationships can be obtained only for sufficiently large sets of the structures $[(A)_nZ-Y\cdots X]^-$ which include different types of second-order atoms Z and third-order groups A, otherwise, the relationships found may suffer a significant overfitting. Therefore, a large statistically significant set of 412 structures bearing twelve different types of the Z atom was used in this work.

2. Computational Details

Full geometry optimization of the main set of structures was carried out at the density functional theory (DFT) level by using the M06-2X functional [121] with the help of the Gaussian 09 [122] program package applying tight optimization criteria and an ultrafine integration grid. Cartesian d and f basis functions (6d, 10f) were used in all calculations. The ADZP basis set taken from the Basis Set Exchange library [123] was applied for geometry optimization. The energies of the equilibrium structures were refined by the second-order scalar relativistic correction using the Douglas–Kroll–Hess method (DKH) and single-point calculations with the ADZP–DKH basis set [123,124]. The ADZP–DKH basis set was constructed from the DZP–DKH basis set [125–127] by addition of diffuse functions taken from the ADZP basis set.

Similar level of theory was applied in the previous work for the analysis of correlations for the $[(A)_nZ-Y\cdots X]^-$ structures ($X, Y = F, Cl, Br$) [116]. It was shown by Kozuch and Martin [128] for a set of 51 structures bearing halogen bonds that the interaction energies calculated with the M06-2X functional correlate well with the reference CCSD(T) level providing the root-mean-square deviation, the mean signed error, and the maximum error of 0.43, 0.01, and 1.58 kcal/mol, respectively. It was also shown [116] that the $E_{\text{int}}(V_b)$ correlations for the $[(A)_nZ-Y\cdots X]^-$ structures ($X, Y = F, Cl, Br$) obtained at the M06-2X level of theory have similar parameters as those for the MP4, CCSD, and CCSD(T) methods. On the other hand, it was found [116] that the simple double-zeta quality basis set 6-31+G* which is similar to ADZP provides the interaction energy values and parameters of the $E_{\text{int}}(V_b)$ correlations close to those obtained at the much more extended triple-zeta basis set 6-311++G(3df,3pd).

The applicability of the M06-2X/ADZP–DKH level of theory for the reproduction of experimental interaction energies and electron densities is additionally discussed below in the Results. For this analysis, the interaction energies and electron density values were calculated at the CCSD, CCSD(T), and PBE0-D3BJ levels of theory. The ADZP–DKH, 6-31+G*, 6-311+G**, and aug-cc-pVTZ basis sets were applied.

The Hessian matrix was calculated for all optimized structures to prove the location of correct minima. No symmetry operations were applied during the calculations. The stability test was performed, and stable solutions were achieved for all structures using the keyword STABLE(OPT).

The interaction energies for the $Y \dots X$ bond in $[(A)_nZ-Y\cdots X]^-$ were calculated using Equation (1):

$$E_{\text{int}} = E([(A)_nZ-Y\cdots X]^-)_{\text{ADZP-DKH}} - E((A)_nZ-Y)_{\text{ADZP-DKH}} - E(X^-)_{\text{ADZP-DKH}} + \text{BSSE}_{\text{ADZP}} \quad (1)$$

where BSSE is a basis set superposition error estimated using the counterpoise (CP) method [129,130] with the ADZP basis set. Geometries of the $(A)_nZ-Y$ fragments were unrelaxed and corresponded to those in $[(A)_nZ-Y\cdots X]^-$. The topological analysis of the electron density distribution was performed with the help of the Atoms in Molecules (AIM) method developed by Bader [131] using the AIMAll program [132].

3. Computational Models

Structures of the $[(A)_nZ-I\cdots X]^-$ and $[(A)_nZ-Y\cdots I]^-$ types ($X = F, Cl, Br, I; Y = Cl, Br, I; Z = F, Cl, Br, I, C, N, O, H, S, P, Si, B$; 412 structures in total) were selected for the calculations.

Among them, 70 structures were in each series $[(A)_nZ-I\cdots X]^-$ with $X = F, Cl,$ or Br and $[(A)_nZ-Br\cdots I]^-$, 65 structures were in the $[(A)_nZ-I\cdots I]^-$ series, and 67 structures were in the $[(A)_nZ-Cl\cdots I]^-$ series. For $Z = C$ and N , different orbital hybridizations of these atoms were considered. For $Z = S$ and P , different oxidation states of these atoms were considered. The groups A (totally 66 groups) vary from the electron donor to the electron acceptor ones providing a broad span of interaction energies for the halogen bond. The complete list of the calculated structures is given in Table S2.

The M06-2X/ADZP-DKH method was validated toward the reproduction of the experimental electron densities for the set of eleven structures bearing halogen bonds of different types ($I \cdots I, Cl \cdots Cl, Br \cdots Cl, Cl \cdots O, Br \cdots Br, I \cdots N,$ and $I \cdots O$) and for which the experimental electron densities are known. Performance of the M06-2X and PBE0-D3BJ functionals was also compared for the set of ten structures of the $[(A)_nZ-I\cdots F]^-$ type ($[Br-I \cdots F]^-$, $[H-I \cdots F]^-$, $[(F_3C)O_2S-I \cdots F]^-$, $[F_3Si-I \cdots F]^-$, $[p-H_2N-C_6H_4-Br-I \cdots F]^-$, $[Me_3Si-I \cdots F]^-$, $[MeO-I \cdots F]^-$, $[(Me)O_2S-I \cdots F]^-$, $[Ph-I \cdots F]^-$, and $[(p-Me-C_6H_4)_2N-I \cdots F]^-$), which provide the E_{int} span from -9 to -73 kcal/mol.

4. Results

4.1. Test of the Computational Method

Since the main goal of this work is to establish relationships between the interaction energy and the experimentally accessible properties such as electron density and derivatives and the length of the halogen bond, it is essential, first, to test the ability of the computational method used to reasonably reproduce these experimental properties. Results of such analysis are presented in this section.

Interaction energy. It is a usual practice to test reliability of a computational method for the estimates of interaction energies against a reference level of theory, such as coupled cluster (CC) approaches. Meanwhile, even the CCSD(T) level often considered as the “gold standard” may be associated with some degree of uncertainty, for instance, due to issues related with the basis set superposition error and its correction [133]. Therefore, when it is possible, experimental data should always be considered as the ultimate reference for method benchmarking.

Here, interaction energies were calculated for several structures bearing the hydrogen or halogen bonds with a halide anion for which experimental data are available (i.e., $H_3C-H\cdots F^-$, $[F-H-F]^-$, $HO-H\cdots Cl^-$, $HO-H\cdots I^-$, $H_3C-H\cdots I^-$, and $[I-I-I]^-$). As can be seen in Table 2, the M06-2X functional with the moderate double-zeta quality basis sets 6-31+G* or ADZP-DKH and the CP correction provide good agreement with the experimental bond energies with the mean absolute deviation (MAD) of 1.2 kcal/mol for the whole set of these structures and of 0.6 kcal/mol excluding $[F-H-F]^-$. The experimental error is in the range of 0.1–1.6 kcal/mol, and theoretical M06-2X values fall within the 3σ interval for four of six structures. The interaction energies calculated at the CCSD and CCSD(T) levels were strongly underestimated when the CP correction was applied. The CCSD method performed worse than M06-2X for $H_3C-H\cdots F^-$ and $HO-H\cdots Cl^-$ even with the aug-cc-pVTZ basis set, and only the CCSD(T) level with the triple-zeta basis set and without the CP correction provided better results than the DFT approach (MAD = 0.3 kcal/mol). Thus, considering that typical MAD values for the E_{int} property relationships found for the structures $[(A)_nZ-Hal_1\cdots Hal_2]^-$ are 2–4 kcal/mol (see [116] and results of this work below), the M06-2X/6-31+G*(or ADZP-DKH) level of theory is reliable for the analysis of interaction energies.

Table 2. Enthalpies of formation of hydrogen and halogen bonds (in kcal/mol).

| Structure | Method | ΔH^a CP/no-CP ^b |
|--|---|---------------------------------------|
| [H ₃ C–H...F] [−] | M06-2X/6-31+G* | −6.8/−7.1 |
| | CCSD/6-31+G* | −4.2/−5.1 |
| | CCSD(T)//CCSD/6-31+G* ^c | −4.3/−5.4 |
| | CCSD/6-311+G** | −4.7/−5.8 |
| | CCSD/aug-cc-pVTZ//6-31+G* ^d | −6.0/−6.4 |
| | CCSD(T)/aug-cc-pVTZ//CCSD/6-31+G* ^e | −6.3/−6.8 |
| | exp. ^f | −6.7 ± 0.2 |
| [F–H–F] [−] | M06-2X/6-31+G* | −50.2/−50.7 |
| | CCSD/6-31+G* | −42.7/−44.8 |
| | CCSD(T)//CCSD/6-31+G* ^c | −42.8/−45.2 |
| | CCSD/6-311+G** | −42.3/−46.5 |
| | CCSD/aug-cc-pVTZ//6-31+G* ^d | −43.7/−45.1 |
| | CCSD(T)/aug-cc-pVTZ//CCSD/6-31+G* ^e | −43.9/−45.4 |
| | CCSD/aug-cc-pVTZ | −44.8/−46.3 |
| CCSD(T)//CCSD/aug-cc-pVTZ ^c | −45.0/−46.6 | |
| exp. ^g | −45.8 ± 1.6 | |
| [HO–H...Cl] [−] | M06-2X/6-31+G* | −15.0/−15.2 |
| | CCSD/6-31+G* | −12.3/−14.2 |
| | CCSD(T)//CCSD/6-31+G* ^c | −12.5/−14.5 |
| | CCSD/aug-cc-pVTZ//6-31+G* ^d | −13.3/−13.9 |
| | CCSD(T)/aug-cc-pVTZ//CCSD/6-31+G* ^e | −13.8/−14.4 |
| | CCSD/aug-cc-pVTZ | −13.5/−14.2 |
| | CCSD(T)//CCSD/aug-cc-pVTZ ^c | −14.0/−14.8 |
| exp. ^h | −14.9 ± 0.2 | |
| [HO–H...I] [−] | M06-2X/ADZP–DKH//ADZP ⁱ | −10.3/−14.0 |
| | CCSD(T)/aug-cc-pVTZ(PP)//CCSD/ADZP ^j | −8.1/−11.0 |
| | exp. ^h | −11.1 ± 0.1 |
| [H ₃ C–H...I] [−] | M06-2X/ADZP–DKH//ADZP ⁱ | −1.6/−3.1 |
| | CCSD(T)/aug-cc-pVTZ(PP)//CCSD/ADZP ^j | −0.4/−2.4 |
| | exp. ^f | −2.6 ± 0.2 |
| [I–I–I] [−] | M06-2X/ADZP–DKH//ADZP ^k | −29.3/−36.6 |
| | CCSD(T)/aug-cc-pVTZ(PP)//CCSD/ADZP ^k | −27.3/−30.6 |
| | exp. ^{l,m} | −30.1 ± 1.4 |

^a The calculated values are adiabatic. ^b CP/no-CP means with/without CP correction. ^c $\Delta H = \Delta E(\text{CCSD(T)}) - \Delta E(\text{CCSD}) + \Delta H(\text{CCSD})$. ^d $\Delta H = \Delta E(\text{CCSD/aug-cc-pVTZ}) - \Delta E(\text{CCSD/6-31+G}^*) + \Delta H(\text{CCSD/6-31+G}^*)$. ^e $\Delta H = \Delta E(\text{CCSD(T)/aug-cc-pVTZ}) - \Delta E(\text{CCSD/6-31+G}^*) + \Delta H(\text{CCSD/6-31+G}^*)$. ^f Ref. [134]. ^g Ref. [135]. ^h Ref. [136]. ⁱ $\Delta H = \Delta E(\text{M06-2X/ADZP–DKH}) - \Delta E(\text{M06-2X/ADZP}) + \Delta H(\text{M06-2X/ADZP})$. ^j $\Delta H = \Delta E(\text{CCSD(T)/aug-cc-pVTZ(PP)}) - \Delta E(\text{CCSD/ADZP}) + \Delta H(\text{CCSD/ADZP})$. ^k Adiabatic interaction energy in terms of E_{int} . ^l Ref. [137]. ^m Enthalpy at 0 K.

Electron density. Recently, it has been shown that the M06-2X functional is not sufficiently good to reproduce the experimental electron density properties for isolated atoms and atomic cations [138]. Here, the ability of this functional to reproduce the experimental ρ_b values was tested for the BCPs corresponding to the halogen bonds in eleven structures (Table 3). The calculated structures corresponded to the experimental X-ray ones. The results indicate that the M06-2X/ADZP–DKH method adequately reproduces the experimental electron density at BCPs in these structures with the MAD and RMSD values of 0.006 and 0.009 e/A³, respectively. The slope of the correlation $\rho_{b,\text{theor}}$ against the experimental values $\rho_{b,\text{exp}}$ was quite close to unity (1.07, Figure S1). The PBE0 functional found by Medvedev et al. [138] as one of the best to reproduce the electron density properties in isolated atoms and atomic cations demonstrates the performance similar to M06-2X for halogen bonds (MAD = 0.006 e/A³, RMSD = 0.009 e/A³, slope, 1.12).

Table 3. Theoretical and experimental electron densities (in $e/\text{Å}^3$) at the corresponding BCP.

| Ref. Code | Contact | $\rho_{b,\text{theor}}$ (M06-2X) | $\rho_{b,\text{theor}}$ (PBE0-D3BJ) | $\rho_{b,\text{exp}}$ [Ref.] |
|-------------|---------|----------------------------------|-------------------------------------|------------------------------|
| ICSD 194468 | I...I | 0.097 | 0.102 | 0.101 [139] |
| ETUDUT01 | Cl...Cl | 0.052 | 0.050 | 0.048(2) [140] |
| IJIGOU | Cl...Cl | 0.033 | 0.032 | 0.03 [141] |
| FUFNOJ02 | Cl...Cl | 0.053 | 0.051 | 0.05 [141] |
| IJIHAL | Cl...Cl | 0.045 | 0.044 | 0.03 [141] |
| CIHBAX01 | Br...Cl | 0.079 | 0.078 | 0.081(2) [142] |
| BZQDCL11 | Cl...O | 0.055 | 0.054 | 0.054(1) [143] |
| PCPHOL01 | Cl...Cl | 0.050 | 0.048 | 0.058 [144] |
| ROFKAZ01 | Br...Br | 0.061 | 0.060 | 0.063 [144] |
| XIPRUL | I...N | 0.174 | 0.176 | 0.154(12) [145] |
| XIPRUL | I...O | 0.099 | 0.105 | 0.092(7) [145] |

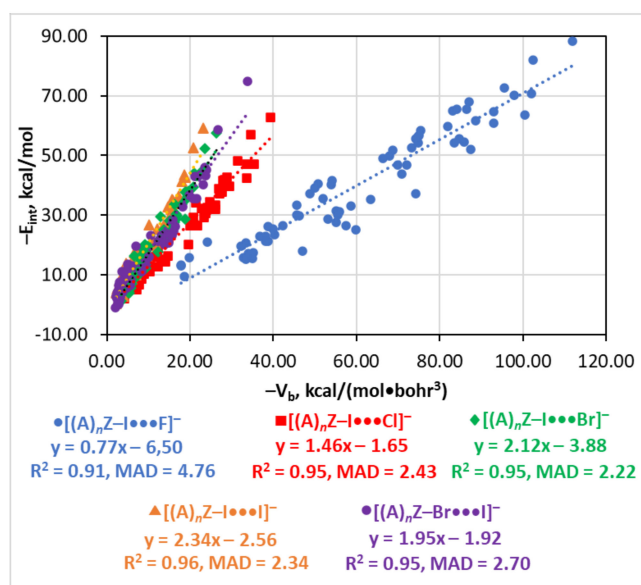
Correspondingly, the $E_{\text{int}}(V_b)$ relationships obtained for the small set of ten structures of the $[(A)_nZ-I\cdots F]^-$ type were similar for both M06-2X and PBE0-D3BJ functionals (Figure S2). The deviation of E_{int} estimated by these two methods was 2.27 kcal/mol at $V_b = 20$ kcal/(mol•bohr³) and it was 3.96 kcal/mol at $V_b = 100$ kcal/(mol•bohr³). These deviations were lower than MAD for the whole set of seventy $[(A)_nZ-I\cdots F]^-$ structures (4.76 kcal/mol, see below). All these results indicate that the relationships found in this work at the M06-2X/ADZP-DKH level are reliable for the determination of E_{int} using experimental electron density properties.

4.2. Interaction Energies

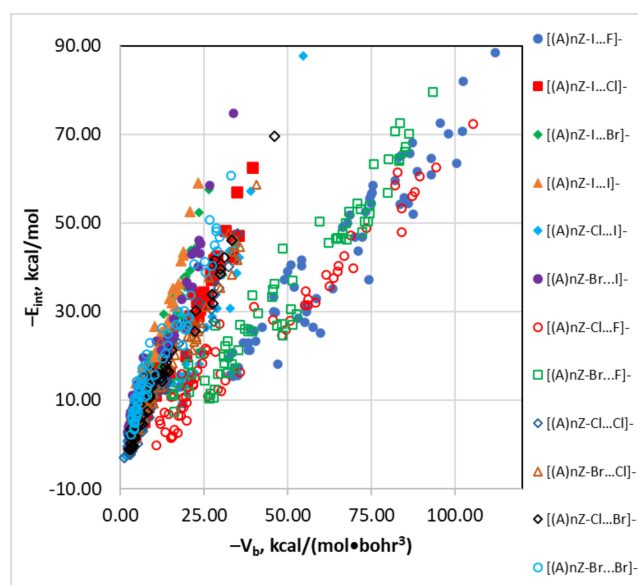
After validation of the computational method, the interaction energies calculated for 412 structures of the $[(A)_nZ-I\cdots X]^-$ and $[(A)_nZ-Y\cdots I]^-$ types and the corresponding E_{int} property relationships were discussed (in this and the following sections). The calculated BSSE-corrected interaction energies for the halogen bonds in these structures varied between 2.53 and −88.43 kcal/mol. These bonds were the strongest for the $[(A)_nZ-I\cdots F]^-$ series. The highest dispersion of E_{int} was found for the $[(A)_nZ-I\cdots F]^-$ and $[(A)_nZ-Cl\cdots I]^-$ series. The halogen bonds in the series $[(A)_nZ-I\cdots Cl]^-$, $[(A)_nZ-I\cdots Br]^-$, and $[(A)_nZ-I\cdots I]^-$ have similar strengths and dispersion.

4.3. The $E_{\text{int}}(V_b)$, $E_{\text{int}}(G_b)$, and $E_{\text{int}}(\rho_b)$ Relationships

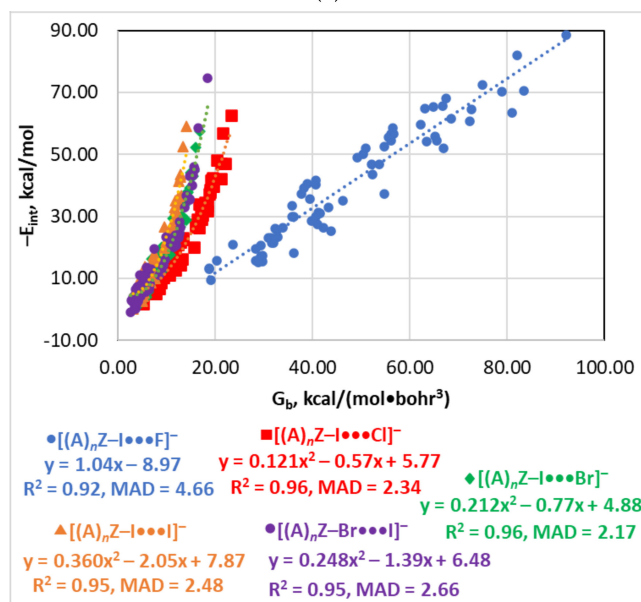
These types of relationships were recommended for the predictions of E_{int} for the hydrogen bonds X–H...O and FH...FR [82,83] and for the halogen bonds $[(A)_nZ-Y\cdots X]^-$ (X, Y = F, Cl, Br) bearing halide anions [116]. Here, the linear correlations between E_{int} and V_b were found for all series except $[(A)_nZ-Cl\cdots I]^-$ (Figure 1). The $E_{\text{int}}(G_b)$ relationship was linear only for the $[(A)_nZ-I\cdots F]^-$ series and it was approximated by a binominal function for $[(A)_nZ-I\cdots X]^-$ (X = Cl, Br, or I) and $[(A)_nZ-Br\cdots I]^-$. Finally, the $E_{\text{int}}(\rho_b)$ dependence was quadratic for all series.



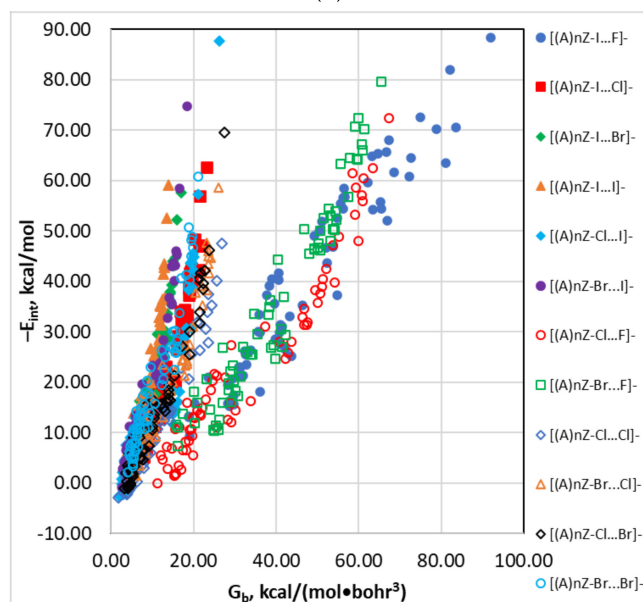
(a)



(b)



(c)



(d)

Figure 1. Cont.

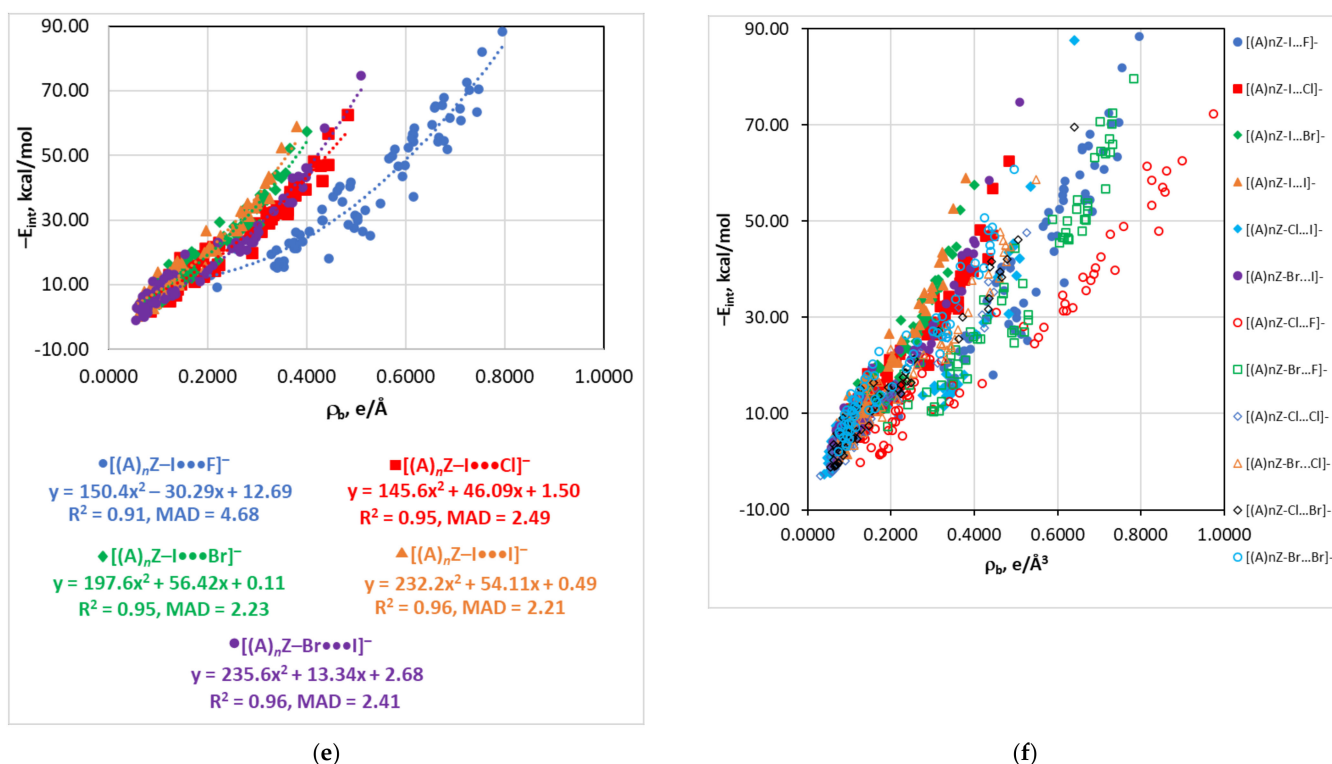


Figure 1. Plots of $-E_{\text{int}}$ against $-V_b$, G_b , and ρ_b for the structures $[(A)_nZ-Y\cdots I]^-$ and $[(A)_nZ-I\cdots X]^-$ (a,c,e) and $[(A)_nZ-Y\cdots X]^-$ (b,d,f); data for the non-iodine structures were taken from [116].

An interesting relationship distinct from all other bonds with halide anions was obtained for the $[(A)_nZ-Cl\cdots I]^-$ series (Figure 2). These structures could not be treated by a single linear or quadratic $E_{\text{int}}(V_b)$, $E_{\text{int}}(G_b)$, or $E_{\text{int}}(\rho_b)$ function. Instead, the horizontal branch is clearly visible in the range of E_{int} of 10–20 kcal/mol. The interaction energy could be reasonably approximated by polynomial fourth-order functions, but such an approximation is usually associated with significant overfitting and cannot be recommended for practical use. The reasons of this peculiar situation are discussed below.

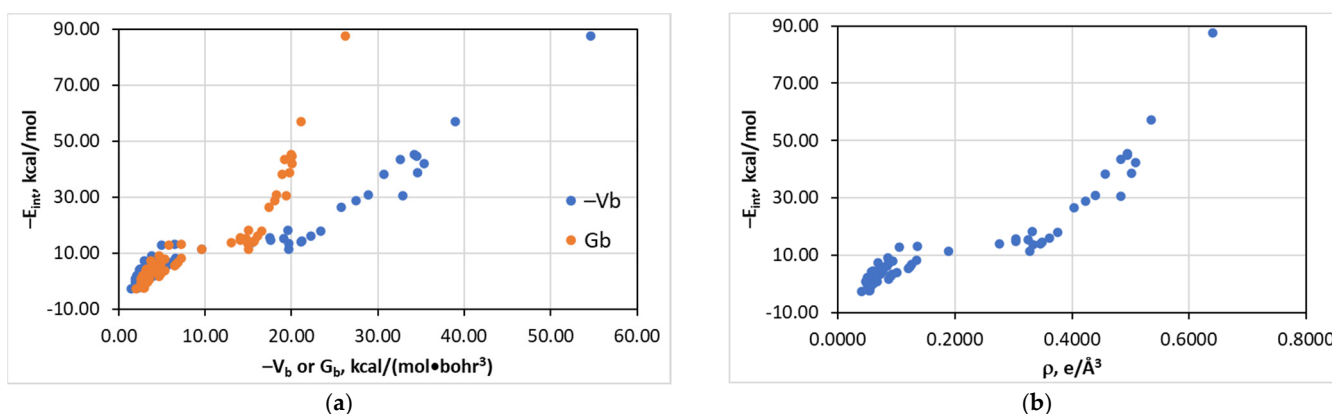


Figure 2. Plots of $-E_{\text{int}}$ against $-V_b$, G_b (a), and ρ_b (b) for the structures $[(A)_nZ-Cl\cdots I]^-$.

Analysis of the relationships obtained for the structures $[(A)_nZ-Y\cdots X]^-$ in this and previous [116] works allows making the following additional conclusions and generalizations. First, all three estimators, V_b , G_b , and ρ_b , behave similarly (Table 4). Second, correlations for the $[(A)_nZ-Y\cdots F]^-$ series ($R^2 = 0.91\text{--}0.95$, $\text{MAD} = 3.29\text{--}4.76$ kcal/mol) are of a lower quality compared to other series ($R^2 = 0.93\text{--}0.96$, $\text{MAD} = 2.06\text{--}3.01$), except $[(A)_nZ-Cl\cdots I]^-$.

Third, the slope of the relationships is strongly affected by the nature of the Y and X atoms. For instance, for the V_b estimator, the lowest slope (0.69–0.84) and the highest negative intercept ($-3.68 \div -6.50$) were found for $X = F$. The highest slopes were detected for $[(A)_nZ-I\cdots I]^-$ (2.34) as well as for the $[(A)_nZ-Y\cdots X]^-$ ($Y = Br, X = I; Y = I, X = Br, X = Y = Br$) series (1.55–2.12). The series with $(X \text{ or/and } Y) = Cl$ but $(X \text{ and } Y) \neq F$ exhibited an intermediate slope (1.26–1.46). Such a behavior can be qualitatively interpreted by the different properties of the halogen atoms forming the $Y\cdots X$ bond. First of all, the electronegativity of the X atom decreases along the series $F > Cl > Br > I$. There is a clear trend between the slope of the $E_{int}(V_b)$ dependence and the difference of the electronegativities of X and Y (Figure S3). Thus, the higher the electronegativity difference, the lower the E_{int} at a given energy density at BCP. This conclusion becomes understandable if we recall that ionic bonds have high interaction energies but low electron densities at BCP. The second factor is an enhancement of polarizability, diffuse character of electron shells, and the role of dispersion forces from $X = F$ to I . Electronic effects from the $(A)_nZ$ group on the $Y\cdots X$ bond are more pronounced if the electron shells of X are more diffuse, i.e., from $X = F$ to I . Since the higher dispersion contribution and more diffuse electron shells are associated with lower concentration of electron or energy density at BCP, E_{int} values are higher for most electron acceptor groups $(A)_nZ$ at a given value of E_{int} in the case of heavier atom X.

Table 4. The R^2 and MAD (kcal/mol) values calculated for the V_b , G_b , ρ_b , and $d(Y\cdots X)$ estimators for the series $[(A)_nZ-Y\cdots X]^-$.

| Series | V_b | | G_b | | ρ_b | | $d(Y\cdots X)$ | |
|---------------------------------------|-------|------|-------|------|-------------------|-------------------|----------------|------|
| | R^2 | MAD | R^2 | MAD | R^2 | MAD | R^2 | MAD |
| $[(A)_nZ-I\cdots F]^-$ | 0.91 | 4.76 | 0.92 | 4.66 | 0.91 | 4.68 | 0.91 | 4.77 |
| $[(A)_nZ-Cl\cdots F]^-$ ^a | 0.95 | 3.36 | 0.95 | 3.53 | 0.94 ^b | 3.59 ^b | 0.94 | 3.88 |
| $[(A)_nZ-Br\cdots F]^-$ ^a | 0.94 | 3.83 | 0.95 | 3.29 | 0.94 ^b | 3.73 ^b | 0.93 | 4.00 |
| $[(A)_nZ-I\cdots Cl]^-$ | 0.95 | 2.43 | 0.96 | 2.34 | 0.95 | 2.49 | 0.95 | 2.55 |
| $[(A)_nZ-Cl\cdots Cl]^-$ ^a | 0.95 | 2.06 | 0.95 | 2.08 | 0.95 | 2.15 | 0.95 | 2.17 |
| $[(A)_nZ-Br\cdots Cl]^-$ ^a | 0.94 | 2.73 | 0.94 | 2.63 | 0.93 | 3.01 | 0.94 | 2.78 |
| $[(A)_nZ-Cl\cdots Br]^-$ ^a | 0.96 | 2.17 | 0.95 | 2.31 | 0.95 | 2.35 | 0.96 | 2.33 |
| $[(A)_nZ-Br\cdots Br]^-$ ^a | 0.94 | 2.75 | 0.94 | 2.77 | 0.93 | 3.01 | 0.93 | 2.89 |
| $[(A)_nZ-I\cdots Br]^-$ | 0.95 | 2.22 | 0.96 | 2.17 | 0.95 | 2.23 | 0.95 | 2.29 |
| $[(A)_nZ-I\cdots I]^-$ | 0.96 | 2.34 | 0.95 | 2.48 | 0.96 | 2.21 | 0.96 | 2.27 |
| $[(A)_nZ-Br\cdots I]^-$ | 0.95 | 2.70 | 0.95 | 2.66 | 0.96 | 2.41 | 0.96 | 2.50 |

^a From [116]. ^b The data are for the binominal fittings.

Fourth, some series form distinct groups which can be approximated by a single relationship of a reasonable quality. There are three such groups when considering the $E_{int}(V_b)$ dependence, i.e., (i) $[(A)_nZ-I\cdots I]^- + [(A)_nZ-I\cdots Br]^- + [(A)_nZ-Br\cdots I]^-$, (ii) $[(A)_nZ-I\cdots Cl]^- + [(A)_nZ-Cl\cdots Cl]^- + [(A)_nZ-Br\cdots Cl]^- + [(A)_nZ-Cl\cdots Br]^-$, and (iii) $[(A)_nZ-I\cdots F]^- + [(A)_nZ-Br\cdots F]^- + [(A)_nZ-Cl\cdots F]^-$ groups. Each of them may be approximated by a linear function ($R^2 = 0.93\text{--}0.95$, $MAD = 2.58\text{--}4.45$ kcal/mol). The $E_{int}(G_b)$ and $E_{int}(\rho_b)$ dependences are characterized by a higher dispersion between series. They are more sensitive to the nature of the Y and X atoms and, therefore, such a grouping is not efficient for those relationships.

Fifth, the relationships for any series of the $[(A)_nZ-Y\cdots X]^-$ structures were significantly different from those obtained previously for the hydrogen bonds $X-H \cdots O$ and $FH \cdots FR$ [82,83] and for the neutral halogen bonds [117,119,120] (Table 1).

4.4. The $E_{int}(\nabla^2\rho_b)$ Relationship

The Laplacian of electron density may be used as an estimator of E_{int} only for the $[(A)_nZ-I\cdots F]^-$ (this work) and $[(A)_nZ-Br\cdots F]^-$ [116] series (Figure 3). The relationships for these two series are exponential with the different sign of the exponents. The $E_{int}(\nabla^2\rho_b)$ functions for other series are not well-defined (Figure S4).

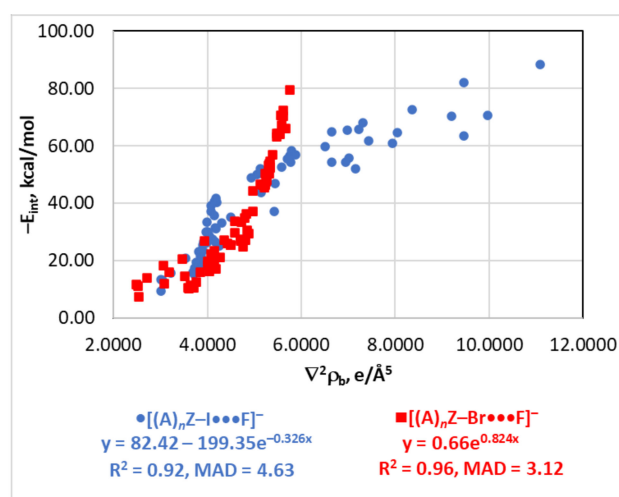


Figure 3. Plots of $-E_{\text{int}}$ against $\nabla^2\rho_b$ for the $[(A)_nZ-I\cdots F]^-$ and $[(A)_nZ-Br\cdots F]^-$ series (data for the $[(A)_nZ-Br\cdots F]^-$ series were taken from [116]).

4.5. The $E_{\text{int}}(\lambda_{||,b})$ Relationship

The curvature of the electron density distribution can serve for the estimates of E_{int} only for three series calculated in this work, i.e., $[(A)_nZ-I\cdots F]^-$, $[(A)_nZ-I\cdots Cl]^-$, and $[(A)_nZ-I\cdots Br]^-$ (Figure 4). The $E_{\text{int}}(\lambda_{||,b})$ relationship for the first of these series is linear and of a lower quality compared to the $E_{\text{int}}(V_b)$, $E_{\text{int}}(G_b)$, and $E_{\text{int}}(\rho_b)$ functions. The last two series are very well approximated by two exponential functions ($R^2 = 0.95\text{--}0.96$, $\text{MAD} = 2.06\text{--}2.51$ kcal/mol). For the series $[(A)_nZ-I\cdots I]^-$ and $[(A)_nZ-Br\cdots I]^-$, the $\lambda_{||,b}$ parameter is not sensitive to determine E_{int} at high values ($E_{\text{int}} > 30$ kcal/mol) (Figure S5). The $E_{\text{int}}(\lambda_{||,b})$ fittings at lower E_{int} are also not reasonable. Finally, the $E_{\text{int}}(\lambda_{||,b})$ function is not well-defined for $[(A)_nZ-Cl\cdots I]^-$.

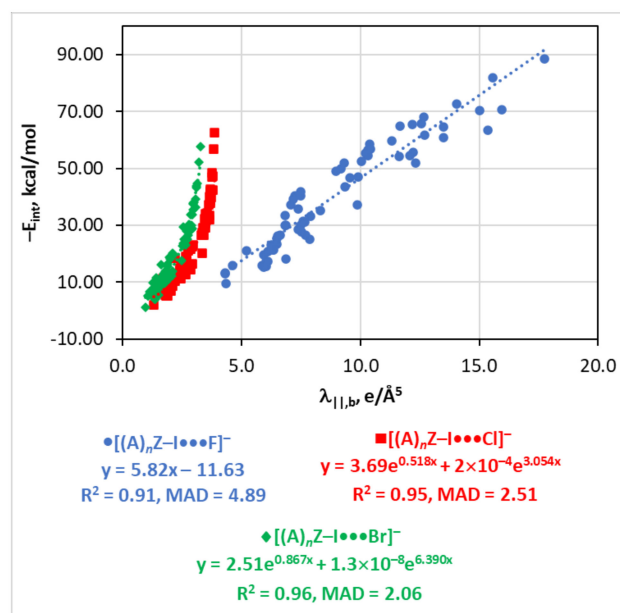


Figure 4. Plots of $-E_{\text{int}}$ against $\lambda_{||,b}$ for the $[(A)_nZ-I\cdots X]^-$ series ($X = F, Cl, Br$).

4.6. The $E_{\text{int}}(H_b)$ Relationship

The quality of the total energy density as an estimator of E_{int} depends on the nature of the Y and X atoms. It cannot be used for the $[(A)_nZ-I\cdots F]^-$ series due to high dispersion of the $E_{\text{int}}(H_b)$ function at lower E_{int} and its low sensitivity at higher E_{int} (Figure S6). For other

series bearing the iodine Y and/or X atom, the $E_{\text{int}}(H_b)$ relationship is not sensitive for the weakest interactions with $E_{\text{int}} < 10$ kcal/mol. However, for stronger interactions, good linear dependences were observed ($R^2 = 0.95$ – 0.96 , $\text{MAD} = 2.07$ – 2.43 kcal/mol), except for the $[(A)_nZ\text{-Cl}\cdots\text{I}]^-$ series which was approximated by a quadratic function ($R^2 = 0.95$, $\text{MAD} = 3.33$ kcal/mol) (Figure 5). Six series (i.e., $[(A)_nZ\text{-I}\cdots\text{Br}]^-$, $[(A)_nZ\text{-I}\cdots\text{I}]^-$, $[(A)_nZ\text{-Br}\cdots\text{I}]^-$, $[(A)_nZ\text{-Cl}\cdots\text{Cl}]^-$, $[(A)_nZ\text{-Cl}\cdots\text{Br}]^-$, and $[(A)_nZ\text{-Br}\cdots\text{Br}]^-$) are described together by a single linear function of the reasonable quality ($R^2 = 0.93$, $\text{MAD} = 2.62$ kcal/mol for $E_{\text{int}} > 10$ kcal/mol) (Figure 5).

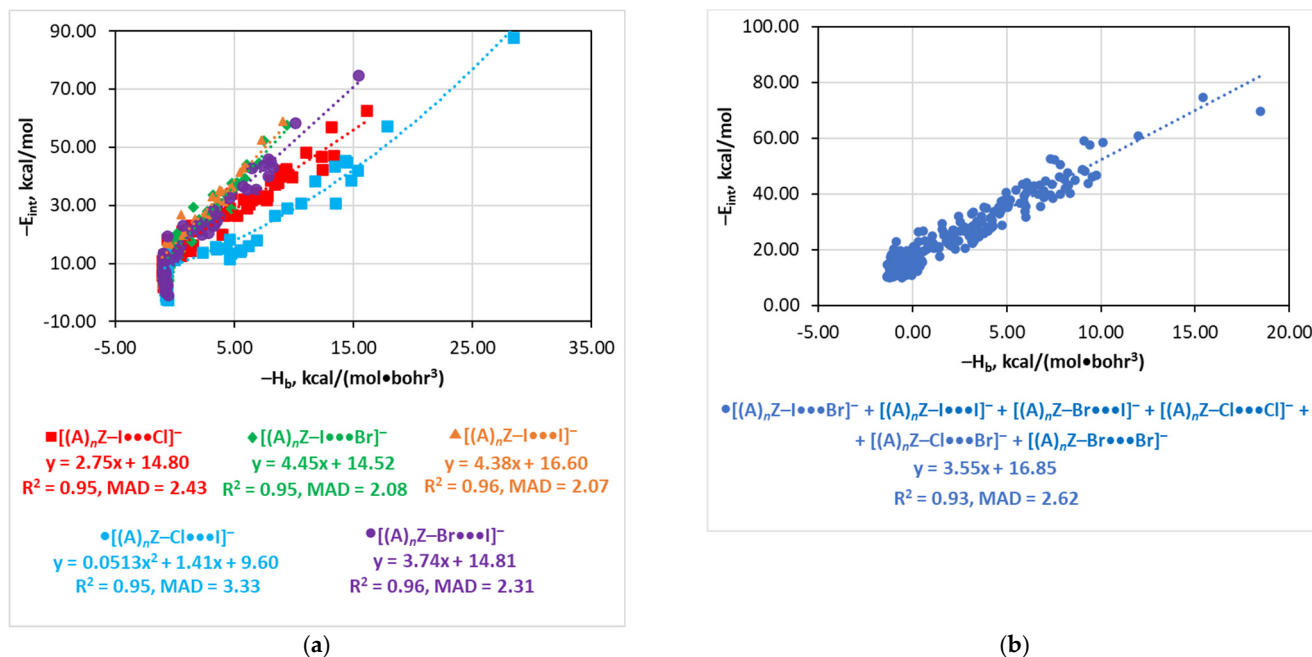


Figure 5. Plots of $-E_{\text{int}}$ against $-H_b$ for the individual $[(A)_nZ\text{-Y}\cdots\text{X}]^-$ series (a) and for the combined set of the structures (b) (the fittings were performed for points corresponding to $-E_{\text{int}} > 10$ kcal/mol, data for the non-iodine structure were taken from [116]).

4.7. The $E_{\text{int}}(d_{Y\dots X})$ Relationship

All series except for $[(A)_nZ\text{-Cl}\cdots\text{I}]^-$ demonstrate reasonable exponential relationships between interaction energy and the length of the halogen bond (Figure 6). The quality of these relationships is similar to those with V_b , G_b , and ρ_b . There are only two couples of series which can be approximated by single correlations, i.e., $[(A)_nZ\text{-I}\cdots\text{Br}]^- + [(A)_nZ\text{-Br}\cdots\text{I}]^-$ and $[(A)_nZ\text{-Br}\cdots\text{Cl}]^- + [(A)_nZ\text{-Cl}\cdots\text{Br}]^-$. For other series, the fitting parameters are quite different from each other. Similarly to the other estimators, the $E_{\text{int}}(d_{Y\dots X})$ dependence is complex for the $[(A)_nZ\text{-Cl}\cdots\text{I}]^-$ series. There is a horizontal branch for the interval of E_{int} 5–15 kcal/mol. Meanwhile, in this case, the dependence may be quite reasonably approximated by a two-exponential function ($R^2 = 0.96$, $\text{MAD} = 2.70$ kcal/mol).

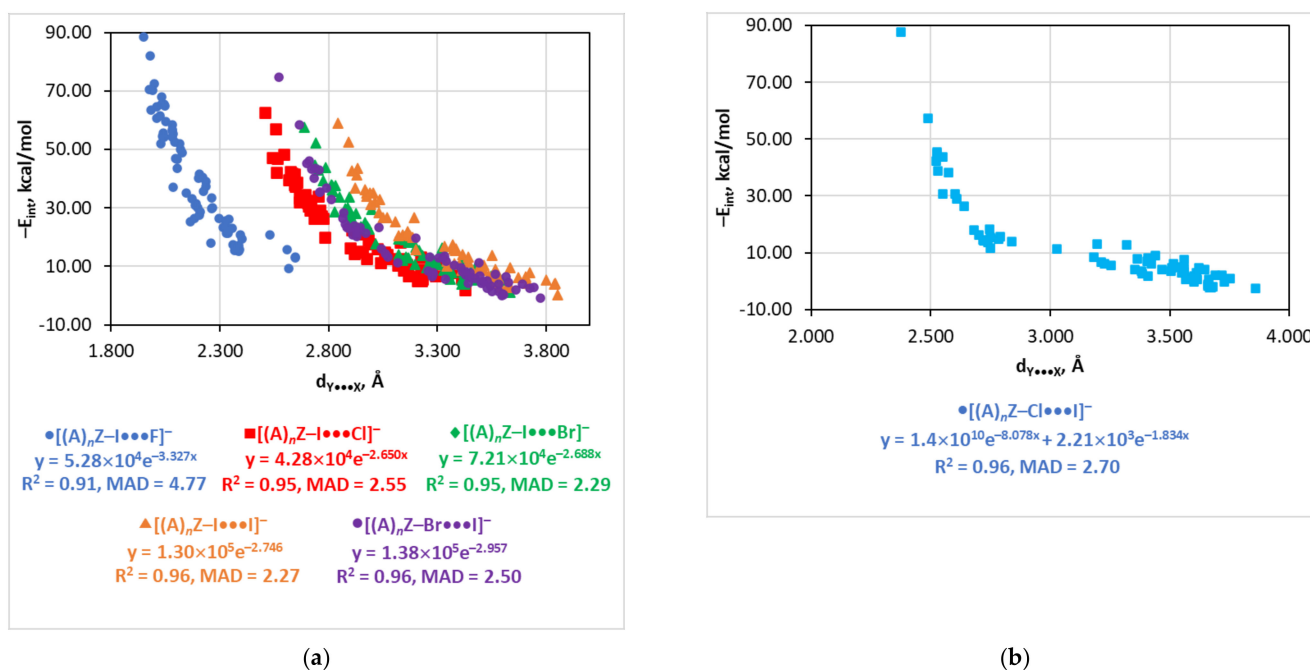


Figure 6. Plots of $-E_{int}$ against $d_{Y...X}$ for the $[(A)_n Z-I \cdots X]^-$, $[(A)_n Z-Br \cdots I]^-$ (a) and $[(A)_n Z-Cl \cdots I]^-$ (b) series.

4.8. The $[(A)_n Z-Cl \cdots I]^-$ Series

As was mentioned above, the E_{int} -property relationships for the $[(A)_n Z-Cl \cdots I]^-$ series have a peculiar character. The more detailed analysis shows that such behavior is due to the tremendous effect of the second-order atom Z and the third-order groups A. First, the E_{int} values are low and do not exceed 14 kcal/mol when Z = C, P, Si, B, or H (Figure 7). The structures with Z = Hal have a relatively high E_{int} (28.95–45.43 kcal/mol) and those with Z = O, N, or S have a significant span of E_{int} (15.26–42.19, 1.70–30.79, and 5.47–87.68 kcal/mol, respectively).

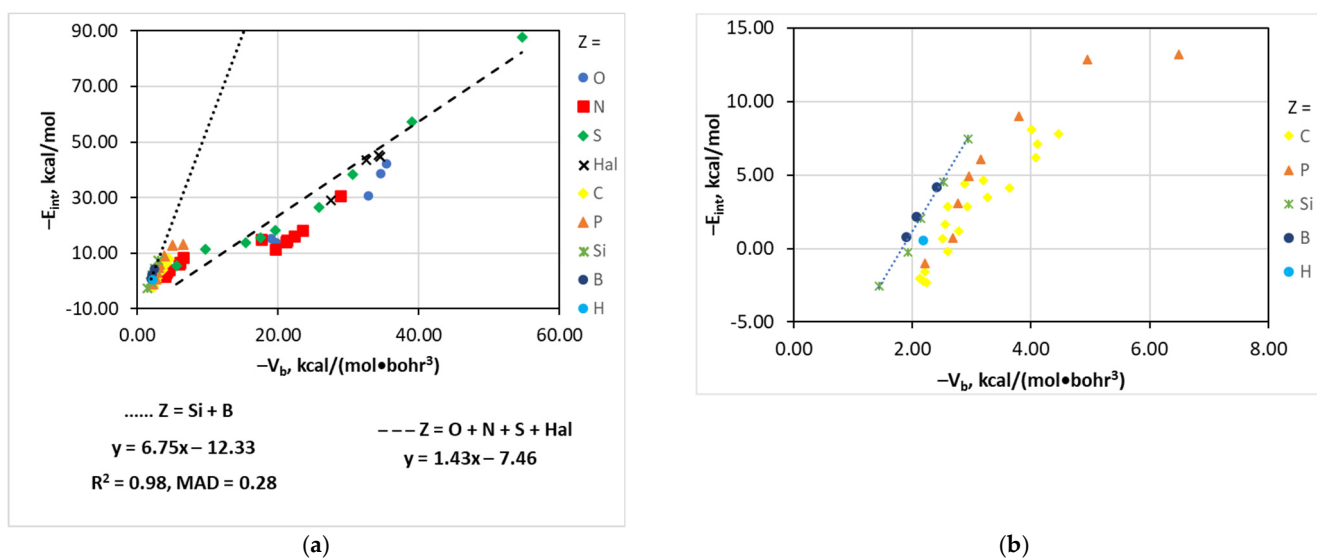


Figure 7. Cont.

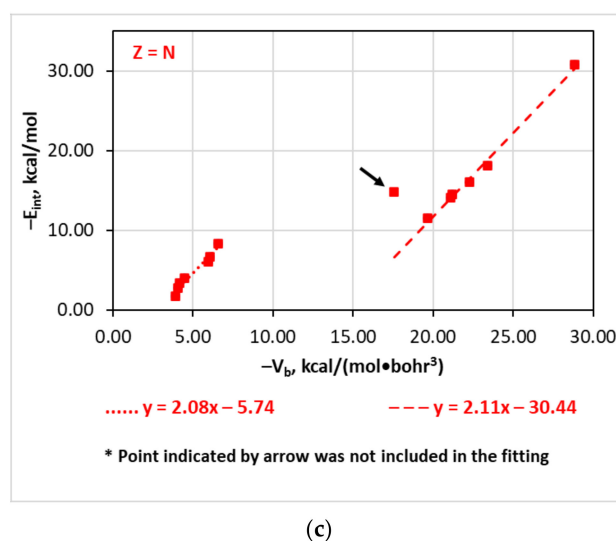


Figure 7. Plots of $-E_{\text{int}}$ against $-V_b$ for the $[(A)_nZ\text{-Cl}\cdots\text{I}]^-$ structures; $Z = \text{Si} + \text{B}$ and $\text{O} + \text{N} + \text{S} + \text{Hal}$ (a), $Z = \text{C}, \text{P}, \text{Si}, \text{B}, \text{H}$ (b), and $Z = \text{N}$ (c).

Second, the $E_{\text{int}}(V_b)$ trend slope for the combined series $[(A)_nZ\text{-Cl}\cdots\text{I}]^-$ ($Z = \text{Si} + \text{B}$) is 6.75 while the slope of the linear correlation for the series $[(A)_nZ\text{-Cl}\cdots\text{I}]^-$ ($Z = \text{O} + \text{N} + \text{S} + \text{Hal}$) is 1.43 (Figure 7). Dependences for the structures $[(A)_nZ\text{-Cl}\cdots\text{I}]^-$ ($Z = \text{P}, \text{C}$) are not linear but exponential. The tangent slopes at the lowest energy points are 9.2 and 8.7.

Third, the $[(A)_n\text{N-Cl}\cdots\text{I}]^-$ structures could be divided into two distinct groups (Figure 7), i.e., structures with a weaker $\text{Cl}\cdots\text{I}$ interaction ($E_{\text{int}} < 10$ kcal/mol, aliphatic and monoaryl amines, methyldiene imine and nitroso compounds, Group I) and those with a stronger $\text{Cl}\cdots\text{I}$ interaction ($E_{\text{int}} > 10$ kcal/mol, diarylamines, difluoro(methyldiene) imine and nitro compounds, Group II). The trend slope for these two groups is similar (2.1) but the intercept is very different (-5.7 and -30.4 , respectively). The different behavior of these two groups is apparently associated with a different nature of the $(A)_n\text{N}$ part of the molecule. In Group I, $(A)_n\text{N}$ exhibits either electron donor or weak electron acceptor properties. In Group II, $(A)_n\text{N}$ is a strong electron acceptor. Furthermore, the structures of Group II have more extended conjugation systems compared to those of Group I. All these relationships considered together provide such a peculiar trend for the whole $[(A)_nZ\text{-Cl}\cdots\text{I}]^-$ series. Interestingly, this effect of Z and A is much smaller for other series making possible the existence of linear correlations. Similar behavior was also found for the G_b and ρ_b estimators.

The great effect of the Z atom and A group on E_{int} does not permit an approximation of the latter via V_b , G_b , or ρ_b for the whole $[(A)_nZ\text{-Cl}\cdots\text{I}]^-$ series. However, for the more narrow series $[(A)_n\text{Si,B-Cl}\cdots\text{I}]^-$, $[(A)_n\text{C-Cl}\cdots\text{I}]^-$, and $[(A)_n\text{P-Cl}\cdots\text{I}]^-$, these relationships are of a good quality ($R^2 = 0.92\text{--}0.98$, $\text{MAD} = 0.28\text{--}0.77$ kcal/mol) and they may be useful for practical applications. The $d(Y \dots X)$ estimator is much better for the description of the $[(A)_nZ\text{-Cl}\cdots\text{I}]^-$ series because it permits the reasonable approximation of E_{int} by a single two-exponent function.

5. Discussion

The estimate of E_{int} for the condensed phases is a much more difficult task than that for the gas phase. Both periodic solid state and cluster approaches often do not allow direct estimates of E_{int} as an energy difference because fragments may have multiple mutual weak intermolecular interactions. When it is possible, the adequate computational model is usually exceedingly large. For instance, accurate calculations of E_{int} for the $A\cdots B$ bond in a solid-state structure within the cluster approach requires explicit consideration of all intermolecular interactions which molecules A and B are involved in. An example of an adequate cluster for the direct estimates of E_{int} between the simple fragments $\text{I-C}_4\text{F}_8\text{-I}$ and

Cl^- in the X-ray structure ACIPOU is shown in Figure S7 and it has 386 atoms (this model is composed of the binuclear cluster $\text{I-C}_4\text{F}_8\text{-I}\cdots\text{Cl}^-$ surrounded by all molecules which form short contacts with the $\text{I-C}_4\text{F}_8\text{-I}$ or Cl^- fragments).

Considering this situation, the practice of utilization of small bimolecular clusters which include only two molecules forming a contact of interest becomes increasingly popular. In other words, there are multiple attempts to approximate the properties of solid-state structures by gas phase calculations.

There are two points which invalidate this practice. First, such a bimolecular model ignores other intermolecular interactions in which both considered molecules participate. These secondary interactions may significantly affect the energy of the contact under study. For instance, E_{int} calculated for the $\text{I-CF}_2\text{CF}_2\text{-I}\cdots\text{Cl}^-$ halogen bond in the X-ray structure ACIPIO using the bimolecular approach is 20.07 kcal/mol. However, when four molecules are considered (three $\text{I-CF}_2\text{CF}_2\text{-I}$ and one Cl^- ion, Figure S8), E_{int} for the $\text{I}\cdots\text{Cl}$ bond becomes 14.75 kcal/mol (see caption to Figure S8 for details) (this structure was taken as one of the examples bearing a short contact between the I atom and the Cl^- ion and where a relatively small cluster may be selected for reliable calculations of the interaction energy).

The second point is that geometry of bimolecular clusters is usually not optimized but taken from the X-ray structures since optimization often leads to the collapse of the structure compared to X-ray. In such calculations, the geometry considered is not equilibrium and does not belong to a minimum energy path for either adiabatic or vertical bond cleavage, and, hence, the resulting E_{int} has little physical meaning.

Application of the correlations established in this work for the rapid estimates of E_{int} in the condensed phase is free from the difficulties discussed above since it requires a single parameter (electron density or halogen bond length) directly obtained from experiment.

6. Final Remarks

In this work, correlations between the halogen bond interaction energy and experimentally accessible properties, i.e., electron density and bond length, were established for the series of structures $[(A)_n\text{Z-I}\cdots\text{Hal}]^-$ and $[(A)_n\text{Z-Hal}\cdots\text{I}]^-$ bearing the iodine atom (412 structures in total). Thus, together with the results published previously [116], this work finalizes the analysis of halogen bonds formed by a halide anion. Obtained correlations are of practical use for rapid estimates of the halogen bond energy in systems with a network of multiple weak interactions. Several concluding remarks and generalizations can be made.

First, among all structures $[(A)_n\text{Z-Y}\cdots\text{X}]^-$, those with $\text{X} = \text{F}$ demonstrate quite poor approximations of E_{int} with MAD of 3.29–4.76 kcal/mol. For other structures, except $[(A)_n\text{Z-Cl}\cdots\text{I}]^-$, more reasonable correlations were obtained (MAD = 2.06–3.01 kcal/mol). Meanwhile, the approximations of E_{int} for halogen bonds formed by halide anions are worse than those obtained for homohalogen bonds formed by two neutral fragments [117].

Second, the most difficult case is the structures of the $[(A)_n\text{Z-Cl}\cdots\text{I}]^-$ type. In fact, only two parameters were found to be able to adequately estimate E_{int} for this bond, i.e., H_b (for strong bonds with negative H_b values) and $d_{\text{Y}\cdots\text{X}}$.

Third, there is no unique equation to approximate E_{int} for all structures $[(A)_n\text{Z-Y}\cdots\text{X}]^-$. For the electron density-based properties, the highest slopes (linear correlations) or curvatures (non-linear correlations) were found for the bonds formed by heavy halogens (I and Br) while the lowest slopes and curvatures were observed for $\text{X} = \text{F}$.

Fourth, the correlations derived for halogen bonds with halide anions are very different from those established for some hydrogen bonds and halogen bonds formed by two neutral fragments (Table 1). This and the previous [116] works indicate that each type of bonding requires the application of its own relationship.

Fifth, the ρ_b , V_b , G_b , and $d_{\text{Y}\cdots\text{X}}$ estimators behave similarly. In contrast, the $\nabla^2\rho_b$, $\lambda_{1|1,b}$, and H_b parameters have limited significance as E_{int} estimators and they may be used only for some series or a certain range of the E_{int} values.

The relationships recommended for practical use to estimate E_{int} of the structures $[(A)_n\text{Z-Y}\cdots\text{I}]^-$ and $[(A)_n\text{Z-I}\cdots\text{X}]^-$ are given in Table 5.

Table 5. Relationships recommended for the estimates of E_{int} (in kcal/mol) for the structures $[(A)_nZ-Y\cdots I]^-$ and $[(A)_nZ-I\cdots X]^-$ at the M06-2X/ADZP-DKH level of theory (V_b , G_b , and H_b in kcal/(mol•bohr³), ρ_b in e/Å³, $\lambda_{||,b}$ in e/Å⁵, $d_{Y\cdots X}$ in Å).

| Series | Estimator | Equation | R ² | MAD |
|----------------------------|-------------------------|---|-------------------------------------|------|
| $[(A)_nZ-I\cdots F]^-$ | V_b | $-E_{\text{int}} = -0.77V_b - 6.50$ | 0.91 | 4.76 |
| | G_b | $-E_{\text{int}} = 1.04G_b - 8.97$ | 0.92 | 4.66 |
| | ρ_b | $-E_{\text{int}} = 150.4\rho_b^2 - 30.29\rho_b + 12.69$ | 0.91 | 4.68 |
| | $d_{Y\cdots X}$ | $-E_{\text{int}} = 5.28 \times 10^4 e^{-3.327d}$ | 0.91 | 4.77 |
| $[(A)_nZ-I\cdots Cl]^-$ | V_b | $-E_{\text{int}} = -1.46V_b - 1.65$ | 0.95 | 2.43 |
| | G_b | $-E_{\text{int}} = 0.121G_b^2 - 0.57G_b + 5.77$ | 0.96 | 2.34 |
| | H_b | $-E_{\text{int}} = -2.75H_b + 14.80^a$ | 0.95 | 2.43 |
| | ρ_b | $-E_{\text{int}} = 145.6\rho_b^2 + 46.09\rho_b + 1.50$ | 0.95 | 2.49 |
| | $\lambda_{ ,b}$ | $-E_{\text{int}} = 3.69e^{0.518\lambda_{ ,b}} + 2 \times 10^{-4}e^{3.054\lambda_{ ,b}}$ | 0.95 | 2.51 |
| $[(A)_nZ-I\cdots Br]^-$ | $d_{Y\cdots X}$ | $-E_{\text{int}} = 4.28 \times 10^4 e^{-2.650d}$ | 0.95 | 2.55 |
| | V_b | $-E_{\text{int}} = -2.12V_b - 3.88$ | 0.95 | 2.22 |
| | G_b | $-E_{\text{int}} = 0.212G_b^2 - 0.77G_b + 4.88$ | 0.96 | 2.17 |
| | H_b | $-E_{\text{int}} = -4.45H_b + 14.52^a$ | 0.95 | 2.08 |
| | ρ_b | $-E_{\text{int}} = 197.6\rho_b^2 + 56.42\rho_b + 0.11$ | 0.95 | 2.23 |
| $[(A)_nZ-I\cdots I]^-$ | $\lambda_{ ,b}$ | $-E_{\text{int}} = 2.51e^{0.867\lambda_{ ,b}} + 1.3 \times 10^{-8}e^{6.390\lambda_{ ,b}}$ | 0.96 | 2.06 |
| | $d_{Y\cdots X}$ | $-E_{\text{int}} = 7.21 \times 10^4 e^{-2.688d}$ | 0.95 | 2.29 |
| | V_b | $-E_{\text{int}} = -2.34V_b - 2.56$ | 0.96 | 2.34 |
| | G_b | $-E_{\text{int}} = 0.360G_b^2 - 2.05G_b + 7.87$ | 0.95 | 2.48 |
| | H_b | $-E_{\text{int}} = -4.38H_b + 16.60^a$ | 0.96 | 2.07 |
| $[(A)_nZ-Cl\cdots I]^-$ | ρ_b | $-E_{\text{int}} = 232.2\rho_b^2 + 54.11\rho_b + 0.49$ | 0.96 | 2.21 |
| | $d_{Y\cdots X}$ | $-E_{\text{int}} = 1.30 \times 10^5 e^{-2.746d}$ | 0.96 | 2.27 |
| | H_b | $-E_{\text{int}} = 0.0513H_b^2 - 1.41H_b + 9.60^a$ | 0.95 | 3.33 |
| | $d_{Y\cdots X}$ | $-E_{\text{int}} = 1.4 \times 10^{10} e^{-8.078d} + 2.21 \times 10^3 e^{-1.834d}$ | 0.96 | 2.70 |
| | $[(A)_nZ-Br\cdots I]^-$ | V_b | $-E_{\text{int}} = -1.95V_b - 1.92$ | 0.95 |
| G_b | | $-E_{\text{int}} = 0.248G_b^2 - 1.39G_b + 6.48$ | 0.95 | 2.66 |
| H_b | | $-E_{\text{int}} = -3.74H_b + 14.81^a$ | 0.96 | 2.31 |
| ρ_b | | $-E_{\text{int}} = 235.6\rho_b^2 + 13.34\rho_b + 2.68$ | 0.96 | 2.41 |
| $d_{Y\cdots X}$ | | $-E_{\text{int}} = 1.38 \times 10^5 e^{-2.957d}$ | 0.96 | 2.50 |
| $[(A)_nP-Cl\cdots I]^-$ | V_b | $-E_{\text{int}} = 14.92 - 68.71e^{0.639V_b}$ | 0.97 | 0.64 |
| $[(A)_nC-Cl\cdots I]^-$ | V_b | $-E_{\text{int}} = 9.84 - 57.41e^{0.725V_b}$ | 0.92 | 0.77 |
| $[(A)_nSi,B-Cl\cdots I]^-$ | V_b | $-E_{\text{int}} = -6.75V_b - 12.33$ | 0.98 | 0.28 |

^a For $E_{\text{int}} > 10$ kcal/mol.

Supplementary Materials: The following are available online: Figure S1: Correlations between theoretical and experimental values of electron density; Figure S2: Correlations between $-E_{\text{int}}$ and $-V_b$ calculated at the M06-2X/ADZP-DKH and PBE0-D3BJ/ADZP-DKH levels of theory; Figure S3: Plot of the slope of the $E_{\text{int}}(V_b)$ dependence against the difference of Pauling's electronegativities of the atoms X and Y; Figures S4–S6: Plots of $-E_{\text{int}}$ against $\nabla^2 \rho_b$, $\lambda_{||,b}$, and H_b ; Figure S7: Example of an adequate cluster for the direct estimates of E_{int} between the fragments I-C₄F₈-I and Cl⁻ in the X-ray structure ACIPOU; Figure S8: Four-molecule computational model of the structure ACIPOU; Table S1: Relationships between interaction energy and electron density-based estimators, Table S2: Calculated structures.

Funding: This research was funded by the Russian Science Foundation (grant No. 19-73-10016) and by Fundação para a Ciência e a Tecnologia (FCT), Portugal (project No. UIDB/00100/2020 of Centro de Química Estrutural).

Data Availability Statement: The data presented in this study are available in supplementary material and from the author upon request.

Acknowledgments: The author is grateful to the Russian Science Foundation (grant No. 19-73-10016) for support of this study (part related to the structures of the $[(A)_nZ-I\cdots I]^-$ type). This work was also partially supported by Fundação para a Ciência e a Tecnologia (FCT), Portugal (project No. UIDB/00100/2020 of Centro de Química Estrutural).

Conflicts of Interest: The author declares no conflict of interest.

References

1. Desiraju, G.R.; Ho, P.S.; Kloo, L.; Legon, A.C.; Marquardt, R.; Metrangolo, P.; Politzer, P.; Resnati, G.; Rissanen, K. Definition of the Halogen Bond (IUPAC Recommendations 2013). *Pure Appl. Chem.* **2013**, *85*, 1711–1713. [[CrossRef](#)]
2. Cavallo, G.; Metrangolo, P.; Milani, R.; Pilati, T.; Priimagi, A.; Resnati, G.; Terraneo, G. The Halogen Bond. *Chem. Rev.* **2016**, *116*, 2478–2601. [[CrossRef](#)] [[PubMed](#)]
3. Metrangolo, P.; Resnati, G. *Halogen Bonding: Fundamentals and Applications*; Springer: Berlin, Germany, 2008.
4. Priimagi, A.; Cavallo, G.; Forni, A.; Gorynsztejn-Leben, M.; Kaivola, M.; Metrangolo, P.; Milani, R.; Shishido, A.; Pilati, T.; Resnati, R.; et al. Halogen Bonding versus Hydrogen Bonding in Driving Self-Assembly and Performance of Light-Responsive Supramolecular Polymers. *Adv. Funct. Mater.* **2012**, *22*, 2572–2579. [[CrossRef](#)]
5. Natale, D.; Marequerivas, J.C. The combination of transition metal ions and hydrogen-bonding interactions. *Chem. Commun.* **2008**, 425–437. [[CrossRef](#)] [[PubMed](#)]
6. Feller, R.K.; Cheetham, A.K. Structural and chemical complexity in multicomponent inorganic–organic framework materials. *CrystEngComm* **2009**, *11*, 980–985. [[CrossRef](#)]
7. Corradi, E.; Meille, S.V.; Messina, M.T.; Metrangolo, P.; Resnati, G. Halogen bonding versus hydrogen bonding in driving self-assembly processes. *Angew. Chem. Int. Ed.* **2000**, *39*, 1782–1786. [[CrossRef](#)]
8. Desiraju, G.R. Crystal engineering: A holistic view. *Angew. Chem. Int. Ed.* **2007**, *46*, 8342–8356. [[CrossRef](#)]
9. Cinčić, D.; Friščić, T.; Jones, W. Structural equivalence of Br and I halogen bonds: A route to isostructural materials with controllable properties. *Chem. Mater.* **2008**, *20*, 6623–6626. [[CrossRef](#)]
10. Tepper, R.; Schubert, U.S. Halogen Bonding in Solution: Anion Recognition, Templated Self-Assembly, and Organocatalysis. *Angew. Chem. Int. Ed.* **2018**, *57*, 6004–6016. [[CrossRef](#)]
11. Mahmudov, K.T.; Kopylovich, M.N.; Guedes da Silva, M.F.C.; Pombeiro, A.J.L. Non-covalent interactions in the synthesis of coordination compounds: Recent advances. *Coord. Chem. Rev.* **2017**, *345*, 54–72. [[CrossRef](#)]
12. Li, B.; Zang, S.-Q.; Wang, L.-Y.; Mak, T.C.W. Halogen bonding: A powerful, emerging tool for constructing high-dimensional metal-containing supramolecular networks. *Coord. Chem. Rev.* **2016**, *308*, 1–21. [[CrossRef](#)]
13. Saccone, M.; Cavallo, G.; Metrangolo, P.; Resnati, G.; Priimagi, A. Halogen-Bonded Photoresponsive Materials. In *Halogen Bonding II. Topics in Current Chemistry*; Metrangolo, P., Resnati, G., Eds.; Springer: Cham, Switzerland, 2014; Volume 359.
14. Aakeröy, C.B.; Spartz, C.L. Halogen Bonding in Supramolecular Synthesis. In *Halogen Bonding I. Topics in Current Chemistry*; Metrangolo, P., Resnati, G., Eds.; Springer: Cham, Switzerland, 2014; Volume 358.
15. Mukherjee, A.; Tothadi, S.; Desiraju, G.R. Halogen bonds in crystal engineering: Like hydrogen bonds yet different. *Acc. Chem. Res.* **2014**, *47*, 2514–2524. [[CrossRef](#)]
16. Cariati, E.; Forni, A.; Biella, S.; Metrangolo, P.; Meyer, F.; Resnati, G.; Righetto, S.; Tordin, E.; Ugo, R. Tuning second-order NLO responses through halogen bonding. *Chem. Commun.* **2007**, 2590–2592. [[CrossRef](#)] [[PubMed](#)]
17. Christopherson, J.-C.; Topić, F.; Barrett, C.J.; Friščić, T. Halogen-Bonded Cocrystals as Optical Materials: Next-Generation Control over Light–Matter Interactions. *Cryst. Growth Des.* **2018**, *18*, 1245–1259. [[CrossRef](#)]
18. Mahmudov, K.T.; Gurbanov, A.V.; Guseinov, F.I.; Guedes da Silva, M.F.C. Noncovalent interactions in metal complex catalysis. *Coord. Chem. Rev.* **2019**, *387*, 32–46. [[CrossRef](#)]
19. Szell, P.M.J.; Zabloutny, S.; Bryce, D.L. Halogen bonding as a supramolecular dynamics catalyst. *Nature Commun.* **2019**, *10*, 916. [[CrossRef](#)] [[PubMed](#)]
20. Schindler, S.; Huber, S.M. Halogen Bonds in Organic Synthesis and Organocatalysis. In *Halogen Bonding II. Topics in Current Chemistry*; Metrangolo, P., Resnati, G., Eds.; Springer: Cham, Switzerland, 2014; Volume 359.
21. Xu, Z.; Yang, Z.; Liu, Y.; Lu, Y.; Chen, K.; Zhu, W. Halogen bond: Its role beyond drug-target binding affinity for drug discovery and development. *J. Chem. Inf. Model.* **2014**, *54*, 69–78. [[CrossRef](#)] [[PubMed](#)]
22. Lu, Y.; Shi, T.; Wang, Y.; Yang, H.; Yan, X.; Luo, X.; Jiang, H.; Zhu, W. Halogen bonding—A novel interaction for rational drug design? *J. Med. Chem.* **2009**, *52*, 2854–2862. [[CrossRef](#)] [[PubMed](#)]
23. Mendez, L.; Henriquez, G.; Sirimulla, S.; Narayan, M. Looking back, looking forward at halogen bonding in drug discovery. *Molecules* **2017**, *22*, 1397. [[CrossRef](#)]
24. Hua, Y.; Flood, A.H. Click chemistry generates privileged CH hydrogen-bonding triazoles: The latest addition to anion supramolecular chemistry. *Chem. Soc. Rev.* **2010**, *39*, 1262–1271. [[CrossRef](#)]
25. Abate, A.; Biella, S.; Cavallo, G.; Meyer, F.; Neukirch, H.; Metrangolo, P.; Pilati, T.; Resnati, G.; Terraneo, G. Halide anions driven self-assembly of haloperfluoroarenes: Formation of one-dimensional non-covalent copolymers. *J. Fluorine Chem.* **2009**, *130*, 1171–1177. [[CrossRef](#)]
26. Dey, B.; Choudhury, S.R.; Gamez, P.; Vargiu, A.V.; Robertazzi, A.; Chen, C.-Y.; Lee, H.M.; Jana, A.D.; Mukhopadhyay, S. Water–Chloride and Water–Bromide Hydrogen-Bonded Networks: Influence of the Nature of the Halide Ions on the Stability of the Supramolecular Assemblies. *J. Phys. Chem. A* **2009**, *113*, 8626–8634. [[CrossRef](#)] [[PubMed](#)]
27. Cowan, J.A. *Supramolecular Chemistry of Anions*; Bianchi, A., Bowman-James, K., Garcoa-Espapa, E., Eds.; Wiley-VCH: New York, NY, USA, 1997.

28. Bowman-James, K. Alfred Werner Revisited: The Coordination Chemistry of Anions. *Acc. Chem. Res.* **2005**, *38*, 671–678. [[CrossRef](#)] [[PubMed](#)]
29. Gale, P.A.; Quesada, R. Anion coordination and anion-templated assembly: Highlights from 2002 to 2004. *Coord. Chem. Rev.* **2006**, *250*, 3219–3244. [[CrossRef](#)]
30. Feiters, M.C.; Meyer-Klaucke, W.; Kostenko, A.V.; Soldatov, A.V.; Leblanc, C.; Michel, G.; Potin, P.; Küpper, F.C.; Hollenstein, K.; Locher, K.P.; et al. Anion binding in biological systems. *J. Phys. Conf. Ser.* **2009**, *190*, 012196. [[CrossRef](#)]
31. Yang, H.S.; Kim, E.; Lee, S.; Park, H.J.; Cooper, D.S.; Rajbhandari, I.; Choi, I. Mutation of Aspartate 555 of the Sodium/Bicarbonate Transporter SLC4A4/NBCE1 Induces Chloride Transport. *J. Biol. Chem.* **2009**, *284*, 15970–15979. [[CrossRef](#)]
32. Okada, Y.; Sato, K.; Numata, T. Pathophysiology and puzzles of the volume-sensitive outwardly rectifying anion channel. *J. Physiol.* **2009**, *587*, 2141–2149.
33. Desiraju, G.R.; Steiner, T. *The Weak Hydrogen Bond in Structural Chemistry and Biology*; Oxford University Press: Oxford, UK, 1999.
34. Sarwar, M.G.; Dragisic, B.; Sagoo, S.; Taylor, M.S. A Tridentate Halogen-Bonding Receptor for Tight Binding of Halide Anions. *Angew. Chem. Int. Ed.* **2010**, *49*, 1674–1677. [[CrossRef](#)]
35. Svec, J.; Necas, M.; Sindelar, V. Bambus [6]uril. *Angew. Chem. Int. Ed.* **2010**, *49*, 2378–2381. [[CrossRef](#)]
36. Chang, K.-J.; Moon, D.; Lah, M.S.; Jeong, K.-S. Indole-Based Macrocycles as a Class of Receptors for Anions. *Angew. Chem. Int. Ed.* **2005**, *44*, 7926–7929. [[CrossRef](#)]
37. Hisaki, I.; Sasaki, S.-I.; Hirose, K.; Tobe, Y. Synthesis and Anion-Selective Complexation of Homobenzyl Tripodal Thiourea Derivatives. *Eur. J. Org. Chem.* **2007**, 607–615. [[CrossRef](#)]
38. Li, Y.; Flood, A.H. Pure C–H Hydrogen Bonding to Chloride Ions: A Preorganized and Rigid Macrocyclic Receptor. *Angew. Chem. Int. Ed.* **2008**, *47*, 2649–2652. [[CrossRef](#)] [[PubMed](#)]
39. Taylor, M.S.; Jacobsen, E.N. Asymmetric Catalysis by Chiral Hydrogen-Bond Donors. *Angew. Chem. Int. Ed.* **2006**, *45*, 1520–1543. [[CrossRef](#)]
40. Lacour, J.; Moraleda, D. Chiral anion-mediated asymmetric ion pairing chemistry. *Chem. Commun.* **2009**, 7073–7089. [[CrossRef](#)] [[PubMed](#)]
41. Hamilton, G.L.; Kanai, T.; Toste, F.D. Chiral Anion-Mediated Asymmetric Ring Opening of meso-Aziridinium and Episulfonium Ions. *J. Am. Chem. Soc.* **2008**, *130*, 14984–14986. [[CrossRef](#)] [[PubMed](#)]
42. Hamilton, G.L.; Kang, E.J.; Mba, M.; Toste, F.D. A Powerful Chiral Counterion Strategy for Asymmetric Transition Metal Catalysis. *Science* **2007**, *317*, 496–499. [[CrossRef](#)] [[PubMed](#)]
43. Coe, B.J.; Fielden, J.; Foxon, S.P.; Brunschwig, B.S.; Asselberghs, I.; Clays, K.; Samoc, A.; Samoc, M. Combining Very Large Quadratic and Cubic Nonlinear Optical Responses in Extended, Tris-Chelate Metallochromophores with Six π -Conjugated Pyridinium Substituents. *J. Am. Chem. Soc.* **2010**, *132*, 3496–3513. [[CrossRef](#)]
44. Leventis, H.C.; O'Mahony, F.; Akhtar, J.; Afzaal, M.; O'Brien, P.; Haque, S.A. Transient Optical Studies of Interfacial Charge Transfer at Nanostructured Metal Oxide/PbS Quantum Dot/Organic Hole Conductor Heterojunctions. *J. Am. Chem. Soc.* **2010**, *132*, 2743–2750. [[CrossRef](#)]
45. Zhao, C.; MacFarlane, D.R.; Bond, A.M. Modified Thermodynamics in Ionic Liquids for Controlled Electrocrystallization of Nanocubes, Nanowires, and Crystalline Thin Films of Silver–Tetracyanoquinodimethane. *J. Am. Chem. Soc.* **2009**, *131*, 16195–16205. [[CrossRef](#)]
46. Wada, H.; de Caro, D.; Valade, L.; Ozawa, T.; Bando, Y.; Mori, T. Thin-film phases of organic charge-transfer complexes formed by chemical vapor deposition. *Thin Solid Films* **2009**, *518*, 299–304. [[CrossRef](#)]
47. Uji, S.; Mori, T.; Takahashi, T. Focus on Organic Conductors. *Sci. Technol. Adv. Mater.* **2009**, *10*, 020301. [[CrossRef](#)]
48. Hodgkiss, J.M.; Tu, G.; Albert-Seifried, S.; Huck, W.T.S.; Friend, R.H. Ion-Induced Formation of Charge-Transfer States in Conjugated Polyelectrolytes. *J. Am. Chem. Soc.* **2009**, *131*, 8913–8921. [[CrossRef](#)] [[PubMed](#)]
49. Williams, J.M.; Wang, H.H.; Emge, T.J.; Geiser, U.; Beno, M.A.; Carlson, R.J.; Thorn, K.D.; Schultz, A.J.; Whangbo, M.-H. Rational Design of Synthetic Metal Superconductors. *Prog. Inorg. Chem.* **1987**, *35*, 51–218.
50. Poreba, T.; Ernst, M.; Zimmer, D.; Macchi, P.; Casati, N. Pressure-Induced Polymerization and Electrical Conductivity of a Polyiodide. *Angew. Chem. Int. Ed.* **2019**, *58*, 6625–6629. [[CrossRef](#)] [[PubMed](#)]
51. Shaw, R.A.; Hill, J.G. A Simple Model for Halogen Bond Interaction Energies. *Inorganics* **2019**, *7*, 19. [[CrossRef](#)]
52. Legon, A.C.; Millen, D.J. Hydrogen bonding as a probe of electron densities: Limiting gas-phase nucleophilicities and electrophilicities of B and HX. *J. Am. Chem. Soc.* **1987**, *109*, 356–358. [[CrossRef](#)]
53. Legon, A.C. A reduced radial potential energy function for the halogen bond and the hydrogen bond in complexes B \cdots XY and B \cdots HX, where X and Y are halogen atoms. *Phys. Chem. Chem. Phys.* **2014**, *16*, 12415–12421. [[CrossRef](#)] [[PubMed](#)]
54. Alkorta, I.; Legon, A.C. Nucleophilicities of Lewis Bases B and Electrophilicities of Lewis Acids A Determined from the Dissociation Energies of Complexes B \cdots A Involving Hydrogen Bonds, Tetrel Bonds, Pnictogen Bonds, Chalcogen Bonds and Halogen Bonds. *Molecules* **2017**, *22*, 1786. [[CrossRef](#)]
55. Afonin, A.V.; Vashchenko, A.V. Benchmark calculations of intramolecular hydrogen bond energy based on molecular tailoring and function-based approaches: Developing hybrid approach. *Int. J. Quant. Chem.* **2019**, *119*, e26001. [[CrossRef](#)]
56. Vologzhanina, A.V.; Buikin, P.A.; Korlyukov, A.A. Peculiarities of Br \cdots Br bonding in crystal structures of polybromides and bromine solvates. *CrystEngComm* **2020**, *22*, 7361–7370. [[CrossRef](#)]

57. Oliveira, V.P.; Marcial, B.L.; Machado, F.B.C.; Kraka, E. Metal-Halogen Bonding Seen through the Eyes of Vibrational Spectroscopy. *Materials* **2020**, *13*, 55. [[CrossRef](#)] [[PubMed](#)]
58. Cao, C.T.; Chen, M.M.; Fang, Z.J.; Au, C.T.; Cao, C.Z. Relationship Investigation between $C(sp^2)-X$ and $C(sp^3)-X$ Bond Energies Based on Substituted Benzene and Methane. *ACS Omega* **2020**, *5*, 19304–19311. [[CrossRef](#)] [[PubMed](#)]
59. Arkhipov, D.E.; Lyubeshkin, A.V.; Volodin, A.D.; Korlyukov, A.A. Molecular Structures Polymorphism the Role of $F\cdots F$ Interactions in Crystal Packing of Fluorinated Tosylates. *Crystals* **2019**, *9*, 242. [[CrossRef](#)]
60. Bartashevich, E.; Matveychuk, Y.; Tsirelson, V. Identification of the Tetrel Bonds between Halide Anions and Carbon Atom of Methyl Groups Using Electronic Criterion. *Molecules* **2019**, *24*, 1083. [[CrossRef](#)] [[PubMed](#)]
61. Mata, I.; Alkorta, I.; Espinosa, E.; Molins, E. Relationships between interaction energy, intermolecular distance and electron density properties in hydrogen bonded complexes under external electric fields. *Chem. Phys. Lett.* **2011**, *507*, 185–189. [[CrossRef](#)]
62. Małecka, M. DFT studies and AIM analysis of intramolecular N–HO hydrogen bonds in 3-aminomethylene-2-methoxy-5,6-dimethyl-2-oxo-2,3-dihydro-2 λ^5 -[1,2]oxaphosphinin-4-one and its derivatives. *Struct. Chem.* **2010**, *21*, 175–184. [[CrossRef](#)]
63. Grabowski, S.J.; Bilewicz, E. Cooperativity halogen bonding effect—Ab initio calculations on $H_2CO\cdots(CIF)_n$ complexes. *Chem. Phys. Lett.* **2006**, *427*, 51–55. [[CrossRef](#)]
64. Szatyłowicz, H. Structural aspects of the intermolecular hydrogen bond strength: H-bonded complexes of aniline, phenol and pyridine derivatives. *J. Phys. Org. Chem.* **2008**, *21*, 897–914. [[CrossRef](#)]
65. Hugas, D.; Simon, S.; Duran, M. Electron Density Topological Properties Are Useful To Assess the Difference between Hydrogen and Dihydrogen Complexes. *J. Chem. Phys. A* **2007**, *111*, 4506–4512. [[CrossRef](#)] [[PubMed](#)]
66. Rozas, I.; Alkorta, I.; Elguero, J. Behavior of Ylides Containing N, O, and C Atoms as Hydrogen Bond Acceptors. *J. Am. Chem. Soc.* **2000**, *122*, 11154–11161. [[CrossRef](#)]
67. Lipkowski, P.; Grabowski, S.J.; Robinson, T.L.; Leszczynski, J. Properties of the C–H \cdots H Dihydrogen Bond: An ab Initio and Topological Analysis. *J. Phys. Chem. A* **2004**, *108*, 10865–10872. [[CrossRef](#)]
68. Grabowski, S.J. Hydrogen bonding strength—measures based on geometric and topological parameters. *J. Phys. Org. Chem.* **2004**, *17*, 18–31. [[CrossRef](#)]
69. Lyssenko, K.A. Analysis of supramolecular architectures: Beyond molecular packing diagrams. *Mendeleev Commun.* **2012**, *22*, 1–7. [[CrossRef](#)]
70. Lyssenko, K.A.; Barzilovich, P.Y.; Nelyubina, Y.V.; Astaf'ev, E.A.; Antipin, M.Y.; Aldoshin, S.M. Charge transfer and hydrogen bond energy in glycinium salts. *Russ. Chem. Bull. Int. Ed.* **2009**, *58*, 31–40. [[CrossRef](#)]
71. Gálvez, O.; Gómez, P.C.; Pacios, L.F. Variation with the intermolecular distance of properties dependent on the electron density in cyclic dimers with two hydrogen bonds. *J. Chem. Phys.* **2003**, *118*, 4878. [[CrossRef](#)]
72. Zou, J.W.; Jiang, Y.-J.; Guo, M.; Hu, G.-X.; Zhang, B.; Liu, H.-C.; Yu, Q.-S. Ab Initio Study of the Complexes of Halogen-Containing Molecules RX ($X = Cl, Br, \text{ and } I$) and NH_3 : Towards Understanding the Nature of Halogen Bonding and the Electron-Accepting Propensities of Covalently Bonded Halogen Atoms. *Chem. Eur. J.* **2005**, *11*, 740–751. [[CrossRef](#)] [[PubMed](#)]
73. Rozenberg, M.; Loewenschuss, A.; Marcus, Y. An empirical correlation between stretching vibration redshift and hydrogen bond length. *Phys. Chem. Chem. Phys.* **2000**, *2*, 2699–2702. [[CrossRef](#)]
74. Pacios, L.F. Change with the Intermolecular Distance of Electron Properties of Hydrogen Bond Dimers at Equilibrium and Non-equilibrium Geometries. *Struct. Chem.* **2005**, *16*, 223–241. [[CrossRef](#)]
75. Raissi, H.; Nadim, E.S.; Yoosefian, M.; Farzad, F.; Ghiamati, E.; Nowroozi, A.R.; Fazli, M.; Amoozadeh, A. The effects of substitutions on structure, electron density, resonance and intramolecular hydrogen bonding strength in 3-mercapto-propenethial. *J. Mol. Struct. Theochem.* **2010**, *960*, 1–9. [[CrossRef](#)]
76. Roohi, H.; Bagheri, S. Influence of substitution on the strength and nature of $CH\cdots N$ hydrogen bond in $XCCH\cdots NH_3$ complexes. *Int. J. Quant. Chem.* **2011**, *111*, 961–969. [[CrossRef](#)]
77. Hayashi, S.; Matsuiwa, K.; Kitamoto, M.; Nakanishi, W. Dynamic Behavior of Hydrogen Bonds from Pure Closed Shell to Shared Shell Interaction Regions Elucidated by AIM Dual Functional Analysis. *J. Phys. Chem. A* **2013**, *117*, 1804–1816. [[CrossRef](#)] [[PubMed](#)]
78. D'Oria, E.; Novoa, J.J. The strength–length relationship at the light of ab initio computations: Does it really hold? *CrystEngComm* **2004**, *6*, 368–376. [[CrossRef](#)]
79. Buralli, G.J.; Petelski, A.N.; Peruchena, N.M.; Sosa, G.L.; Duarte, D.J.R. Multicenter $(FX)_n/NH_3$ Halogen Bonds ($X = Cl, Br$ and $n = 1-5$). QTAIM Descriptors of the Strength of the $X\cdots N$ Interaction. *Molecules* **2017**, *22*, 2034. [[CrossRef](#)]
80. Bartashevich, E.V.; Matveychuk, Y.V.; Mukhitdinova, S.E.; Sobalev, S.A.; Khrenova, M.G.; Tsirelson, V.G. The common trends for the halogen, chalcogen, and pnictogen bonds via sorting principles and local bonding properties. *Theor. Chem. Acc.* **2020**, *139*, 26. [[CrossRef](#)]
81. Boyd, R.J.; Choi, S.C. Hydrogen bonding between nitriles and hydrogen halides and the topological properties of molecular charge distributions. *Chem. Phys. Lett.* **1986**, *129*, 62–65. [[CrossRef](#)]
82. Espinosa, E.; Molins, E.; Lecomte, C. Hydrogen bond strengths revealed by topological analyses of experimentally observed electron densities. *Chem. Phys. Lett.* **1998**, *285*, 170–173. [[CrossRef](#)]
83. Mata, I.; Molins, E.; Alkorta, I.; Espinosa, E. Effect of an external electric field on the dissociation energy and the electron density properties: The case of the hydrogen bonded dimer $HF\cdots HF$. *J. Chem. Phys.* **2009**, *130*, 044104. [[CrossRef](#)]

84. Espinosa, E.; Alkorta, I.; Elguero, J.; Molins, E. From weak to strong interactions: A comprehensive analysis of the topological and energetic properties of the electron density distribution involving X-H...F-Y systems. *J. Chem. Phys.* **2002**, *117*, 5529–5542. [[CrossRef](#)]
85. Parthasarathi, R.; Subramanian, V.; Sathyamurthy, N. Hydrogen bonding without borders: An atoms-in-molecules perspective. *J. Phys. Chem. A* **2006**, *110*, 3349–3351. [[CrossRef](#)]
86. Vener, M.V.; Egorova, A.N.; Churakov, A.V.; Tsirelson, V.G. Intermolecular hydrogen bond energies in crystals evaluated using electron density properties: DFT computations with periodic boundary conditions. *J. Comput. Chem.* **2012**, *33*, 2303–2309. [[CrossRef](#)]
87. Levina, E.O.; Chernyshov, I.Y.; Voronin, A.P.; Alekseiko, L.N.; Stash, A.I.; Vener, M.V. Solving the enigma of weak fluorine contacts in the solid state: A periodic DFT study of fluorinated organic crystals. *RSC Adv.* **2019**, *9*, 12520–12537. [[CrossRef](#)]
88. Ivanov, D.M.; Novikov, A.S.; Ananyev, I.V.; Kirina, Y.V.; Kukushkin, V.Y. Halogen bonding between metal centers and halocarbons. *Chem. Commun.* **2016**, *52*, 5565–5568. [[CrossRef](#)]
89. Romanova, A.; Lyssenko, K.; Ananyev, I. Estimations of Energy of Noncovalent Bonding from Integrals over Interatomic Zero-Flux Surfaces: Correlation Trends and Beyond. *J. Comput. Chem.* **2018**, *39*, 1607–1616. [[CrossRef](#)]
90. Saleh, G.; Gatti, C.; Presti, L.L.; Contreras-García, J. Revealing Non-covalent Interactions in Molecular Crystals through Their Experimental Electron Densities. *Chem. Eur. J.* **2012**, *18*, 15523–15536. [[CrossRef](#)]
91. Esrafilii, M.D.; Ahmadi, B. A theoretical investigation on the nature of Cl...N and Br...N halogen bonds in F-Ar-X...NCY complexes (X = Cl, Br and Y = H, F, Cl, Br, OH, NH₂, CH₃ and CN). *Comput. Theor. Chem.* **2012**, *997*, 77–82. [[CrossRef](#)]
92. Mata, I.; Alkorta, I.; Molins, E.; Espinosa, E. Universal Features of the Electron Density Distribution in Hydrogen-Bonding Regions: A Comprehensive Study Involving H...X (X = H, C, N, O, F, S, Cl, π) Interactions. *Chem. Eur. J.* **2010**, *16*, 2442–2452. [[CrossRef](#)] [[PubMed](#)]
93. Emamian, S.; Lu, T.; Kruse, H.; Emamian, H. Exploring Nature and Predicting Strength of Hydrogen Bonds: A Correlation Analysis between Atoms-in-Molecules Descriptors, Binding Energies, and Energy Components of Symmetry-Adapted Perturbation Theory. *J. Comput. Chem.* **2019**, *40*, 2868–2881. [[CrossRef](#)]
94. de Oliveira, B.G.; Zabardasti, A.; do Rego, D.G.; Pour, M.M. The formation of H...X hydrogen bond, C...X carbon-halide or Si...X tetrel bonds on the silylene-halogen dimers (X = F or Cl): Intermolecular strength, molecular orbital interactions and prediction of covalency. *Theor. Chem. Acc.* **2020**, *139*, 131. [[CrossRef](#)]
95. Boyd, R.J.; Choi, S.C. A bond-length-bond-order relationship for intermolecular interactions based on the topological properties of molecular charge distributions. *Chem. Phys. Lett.* **1985**, *120*, 80–85. [[CrossRef](#)]
96. M \acute{o} , O.; Y \acute{a} ñez, M.; Elguero, J. Cooperative (nonpairwise) effects in water trimers: An ab initio molecular orbital study. *J. Chem. Phys.* **1992**, *97*, 6628. [[CrossRef](#)]
97. Ebrahimi, A.; Khorassani, S.M.H.; Delarami, H. Estimation of individual binding energies in some dimers involving multiple hydrogen bonds using topological properties of electron charge density. *Chem. Phys.* **2009**, *365*, 18–23. [[CrossRef](#)]
98. Koch, U.; Popelier, P.L.A. Characterization of C-H-O Hydrogen Bonds on the Basis of the Charge Density. *J. Phys. Chem.* **1995**, *99*, 9747–9754. [[CrossRef](#)]
99. Amezaga, N.J.M.; Pamies, S.C.; Peruchena, N.M.; Sosa, G.L. Halogen Bonding: A Study based on the Electronic Charge Density. *J. Phys. Chem. A* **2010**, *114*, 552–562. [[CrossRef](#)]
100. Grabowski, S.J. What Is the Covalency of Hydrogen Bonding? *Chem. Rev.* **2011**, *111*, 2597–2625. [[CrossRef](#)]
101. Nikolaienko, T.Y.; Bulavina, L.A.; Hovorun, D.M. Bridging QTAIM with vibrational spectroscopy: The energy of intramolecular hydrogen bonds in DNA-related biomolecules. *Phys. Chem. Chem. Phys.* **2012**, *14*, 7441–7447. [[CrossRef](#)]
102. Porta, P.D.; Zanasi, R.; Monaco, G. Hydrogen–hydrogen bonding: The current density perspective. *J. Comput. Chem.* **2015**, *36*, 707–716. [[CrossRef](#)] [[PubMed](#)]
103. Poater, J.; Fradera, X.; Solà, M.; Duran, M.; Simon, S. On the electron-pair nature of the hydrogen bond in the framework of the atoms in molecules theory. *Chem. Phys. Lett.* **2003**, *369*, 248–255. [[CrossRef](#)]
104. D’Oria, E.; Novoa, J.J. Cation–Anion Hydrogen Bonds: A New Class of Hydrogen Bonds That Extends Their Strength beyond the Covalent Limit. A Theoretical Characterization. *J. Phys. Chem. A* **2011**, *115*, 13114–13123. [[CrossRef](#)] [[PubMed](#)]
105. Shi, F.-Q.; An, J.-J.; Yu, J.-Y. Theoretical Study on Measure of Hydrogen Bonding Strength: R–CN...pyrrole Complexes. *Chin. J. Chem.* **2005**, *23*, 400–403.
106. Cubero, E.; Orozco, M.; Hobza, P.; Luque, F.J. Hydrogen Bond versus Anti-Hydrogen Bond: A Comparative Analysis Based on the Electron Density Topology. *J. Phys. Chem. A* **1999**, *103*, 6394–6401. [[CrossRef](#)]
107. Parthasarathi, R.; Subramanian, V.; Sathyamurthy, N. Hydrogen Bonding in Phenol, Water, and Phenol–Water Clusters. *J. Phys. Chem. A* **2005**, *109*, 843–850. [[CrossRef](#)]
108. Wojtulewski, S.; Grabowski, S.J. Unconventional F–H... π hydrogen bonds—ab initio and AIM study. *J. Molec. Struct.* **2002**, *605*, 235–240. [[CrossRef](#)]
109. Bagheri, S.; Masoodi, H.R.; Abadi, M.N. Estimation of individual NH...X (X = N, O) hydrogen bonding energies in some complexes involving multiple hydrogen bonds using NBO calculations. *Theor. Chem. Acc.* **2015**, *134*, 127. [[CrossRef](#)]
110. Jabłonski, M.; Solà, M. Influence of Confinement on Hydrogen Bond Energy. The Case of the FH...NCH Dimer. *J. Phys. Chem. A* **2010**, *114*, 10253–10260. [[CrossRef](#)]

111. Ayoub, A.T.; Tuszynski, J.; Klobukowski, M. Estimating hydrogen bond energies: Comparison of methods. *Theor. Chem. Acc.* **2014**, *133*, 1520. [[CrossRef](#)]
112. Brovarets, O.O.; Yurenko, Y.P.; Hovorun, D.M. Intermolecular CH \cdots O/N H-bonds in the biologically important pairs of natural nucleobases: A thorough quantum-chemical study. *J. Biomol. Struct. Dyn.* **2014**, *32*, 993–1022. [[CrossRef](#)]
113. Martyniak, A.; Majerz, I.; Filarowski, A. Peculiarities of quasi-aromatic hydrogen bonding. *RSC Adv.* **2012**, *2*, 8135–8144. [[CrossRef](#)]
114. Iogansen, A.V. Direct Proportionality of the Hydrogen Bonding Energy and the Intensification of the Stretching ν (XH) Vibration in Infrared Spectra. *Spectrochim. Acta A* **1999**, *55*, 1585–1612. [[CrossRef](#)]
115. Alkorta, I.; Legon, A.C. An Ab Initio Investigation of the Geometries and Binding Strengths of Tetrel-, Pnictogen-, and Chalcogen-Bonded Complexes of CO₂, N₂O, and CS₂ with Simple Lewis Bases: Some Generalizations. *Molecules* **2018**, *23*, 2250. [[CrossRef](#)] [[PubMed](#)]
116. Kuznetsov, M.L. Can halogen bond energy be reliably estimated from electron density properties at bond critical point? The case of the (A)_nZ Y \cdots X[−] (X, Y = F, Cl, Br) interactions. *Int. J. Quant. Chem.* **2019**, *119*, e25869. [[CrossRef](#)]
117. Kuznetsov, M.L. Relationships between Interaction Energy and Electron Density Properties for Homo Halogen Bonds of the [(A)_nY–X \cdots X–Z(B)_m] Type (X = Cl, Br, I). *Molecules* **2019**, *24*, 2733. [[CrossRef](#)] [[PubMed](#)]
118. Spackman, M.A. How Reliable Are Intermolecular Interaction Energies Estimated from Topological Analysis of Experimental Electron Densities? *Cryst. Growth Des.* **2015**, *15*, 5624–5628. [[CrossRef](#)]
119. Bartashevich, E.V.; Tsirelson, V.G. Interplay between non-covalent interactions in complexes and crystals with halogen bonds. *Russ. Chem. Rev.* **2014**, *83*, 1181–1203. [[CrossRef](#)]
120. Bauzá, A.; Frontera, A. Halogen and Chalcogen Bond Energies Evaluated Using Electron Density Properties. *ChemPhysChem* **2020**, *21*, 26–31. [[CrossRef](#)] [[PubMed](#)]
121. Zhao, Y.; Truhlar, D.G. The M06 suite of density functionals for main group thermochemistry, thermochemical kinetics, noncovalent interactions, excited states, and transition elements: Two new functionals and systematic testing of four M06-class functionals and 12 other functionals. *Theor. Chem. Acc.* **2008**, *120*, 215–241.
122. *Gaussian 09*; Frisch, M.J., Trucks, G.W., Schlegel, H.B., Scuseria, G.E., Robb, M.A., Cheeseman, J.R., Scalmani, G., Barone, V., Mennucci, B., Petersson, G.A., et al., Eds.; Revision D.01; Gaussian: Wallingford, CT, USA, 2013.
123. Pritchard, B.P.; Altarawy, D.; Didier, B.; Gibson, T.D.; Windus, T.L. A New Basis Set Exchange: An Open, Up-to-date Resource for the Molecular Sciences Community. *J. Chem. Inf. Model.* **2019**, *59*, 4814–4820. [[CrossRef](#)]
124. Jorge, F.E.; Canal Neto, A.; Camiletti, G.G.; Machado, S.F. Contracted Gaussian basis sets for Douglas–Kroll–Hess calculations: Estimating scalar relativistic effects of some atomic and molecular properties. *J. Chem. Phys.* **2009**, *130*, 064108. [[CrossRef](#)]
125. Neto, A.C.; Muniz, E.P.; Centoducatte, R.; Jorge, F.E. Gaussian basis sets for correlated wave functions. Hydrogen, helium, first- and second-row atoms. *J. Mol. Struct. Theochem.* **2005**, *718*, 219–224. [[CrossRef](#)]
126. Camiletti, G.G.; Machado, S.F.; Jorge, F.E. Gaussian basis set of double zeta quality for atoms K through Kr: Application in DFT calculations of molecular properties. *J. Comp. Chem.* **2008**, *29*, 2434–2444. [[CrossRef](#)]
127. Barros, C.L.; De Oliveira, P.J.P.; Jorge, F.E.; Neto, A.C.; Campos, M. Gaussian basis set of double zeta quality for atoms Rb through Xe: Application in non-relativistic and relativistic calculations of atomic and molecular properties. *Mol. Phys.* **2010**, *108*, 1965–1972. [[CrossRef](#)]
128. Kozuch, S.; Martin, J.M.L. Halogen bonds: Benchmarks and theoretical analysis. *J. Chem. Theory Comput.* **2013**, *9*, 1918–1931. [[CrossRef](#)] [[PubMed](#)]
129. Boys, S.F.; Bernardi, F. The calculation of small molecular interactions by the differences of separate total energies. Some procedures with reduced errors. *Mol. Phys.* **1970**, *19*, 553–566. [[CrossRef](#)]
130. Simon, S.; Duran, M.; Dannenberg, J.J.J. How does basis set superposition error change the potential surfaces for hydrogen-bonded dimers? *Chem. Phys.* **1996**, *105*, 11024–11031. [[CrossRef](#)]
131. Bader, R.F.W. *Atoms in Molecules: A Quantum Theory*; Oxford University Press: Oxford, UK, 1990.
132. Keith, T.A.; Gristmill, T.K. *AIMAll*; Version 14.10.27; Gristmill Software: Overland Park, KS, USA, 2014; Available online: Aim.tkgristmill.com (accessed on 1 September 2015).
133. Burns, L.A.; Marshall, M.S.; Sherrill, C.D. Comparing Counterpoise-Corrected, Uncorrected, and Averaged Binding Energies for Benchmarking Noncovalent Interactions. *J. Chem. Theor. Comput.* **2014**, *10*, 49–57. [[CrossRef](#)] [[PubMed](#)]
134. Hiraoka, K.; Mizuno, T.; Iino, T.; Eguchi, D.; Yamabe, S. Characteristic Changes of Bond Energies for Gas-Phase Cluster Ions of Halide Ions with Methane and Chloromethanes. *J. Phys. Chem. A* **2001**, *105*, 4887–4893. [[CrossRef](#)]
135. Wenthold, P.G.; Squires, R.R. Bond dissociation energies of F₂[−] and HF₂[−]. A gas-phase experimental and G2 theoretical study. *J. Chem. Phys.* **1995**, *99*, 2002–2005.
136. Keesee, R.G.; Castleman, A.W., Jr. Gas-phase studies of hydration complexes of Cl[−] and I[−] and comparison to electrostatic calculations in the gas phase. *Chem. Phys. Lett.* **1980**, *74*, 139–142. [[CrossRef](#)]
137. Do, K.; Klein, T.P.; Pommerening, C.A.; Sunderlin, L.S. A new flowing afterglow-guided ion beam tandem mass spectrometer. Applications to the thermochemistry of polyiodide ions. *J. Am. Soc. Mass Spectrom.* **1997**, *8*, 688–696. [[CrossRef](#)]
138. Medvedev, M.G.; Bushmarinov, I.S.; Sun, J.; Perdew, J.P.; Lyssenko, K.A. Density functional theory is straying from the path toward the exact functional. *Science* **2017**, *355*, 49–52. [[CrossRef](#)]

139. Bertolotti, F.; Shishkina, A.V.; Forni, A.; Gervasio, G.; Stash, A.I.; Tsirelson, V.G. Intermolecular Bonding Features in Solid Iodine. *Cryst. Growth Des.* **2014**, *14*, 3587–3595. [[CrossRef](#)]
140. Wang, R.; Dols, T.S.; Lehmann, C.W.; Englert, U. Charge Density of Intra- and Intermolecular Halogen Contacts. *Z. Anorg. Allg. Chem.* **2013**, *639*, 1933–1939. [[CrossRef](#)]
141. Hathwar, V.R.; Row, T.N.G. Nature of Cl...Cl Intermolecular Interactions via Experimental and Theoretical Charge Density Analysis: Correlation of Polar Flattening Effects with Geometry. *J. Phys. Chem. A* **2010**, *114*, 13434–13441. [[CrossRef](#)]
142. Wang, A.; Wang, R.; Kalf, I.; Dreier, A.; Lehmann, C.W.; Englert, U. Charge-Assisted Halogen Bonds in Halogen-Substituted Pyridinium Salts: Experimental Electron Density. *Cryst. Growth Des.* **2017**, *17*, 2357–2364. [[CrossRef](#)]
143. Hathwar, V.R.; Gonnade, R.G.; Munshi, P.; Bhadbhade, M.M.; Row, T.N.G. Halogen Bonding in 2,5-Dichloro-1,4-benzoquinone: Insights from Experimental and Theoretical Charge Density Analysis. *Cryst. Growth Des.* **2011**, *11*, 1855–1862. [[CrossRef](#)]
144. Brezgunova, M.E.; Aubert, E.; Dahaoui, S.; Fertey, P.; Lebègue, S.; Jelsch, C.; Ángyán, J.G.; Espinosa, E. Charge Density Analysis and Topological Properties of Hal₃-Synthons and Their Comparison with Competing Hydrogen Bonds. *Cryst. Growth Des.* **2012**, *12*, 5373–5386. [[CrossRef](#)]
145. Merkens, C.; Pan, F.; Englert, U. 3-(4-Pyridyl)-2,4-pentanedione—A bridge between coordinative, halogen, and hydrogen bonds. *CrystEngComm* **2013**, *15*, 8153–8158. [[CrossRef](#)]